Microbial Cell Factories

RESEARCH

Open Access

Novel prokaryotic system employing previously unknown nucleic acids-based receptors

Victor Tetz and George Tetz*

Abstract

The present study describes a previously unknown universal system that orchestrates the interaction of bacteria with the environment, named the Teazeled receptor system (TR-system). The identical system was recently discovered within eukaryotes. The system includes DNA- and RNA-based molecules named "TezRs", that form receptor's network located outside the membrane, as well as reverse transcriptases and integrases. TR-system takes part in the control of all major aspects of bacterial behavior, such as intra cellular communication, growth, biofilm formation and dispersal, utilization of nutrients including xenobiotics, virulence, chemo- and magnetoreception, response to external factors (e.g., temperature, UV, light and gas content), mutation events, phage-host interaction, and DNA recombination activity. Additionally, it supervises the function of other receptor-mediated signaling pathways. Importantly, the TR-system is responsible for the formation and maintenance of cell memory to preceding cellular events, as well the ability to "forget" preceding events. Transcriptome and biochemical analysis revealed that the loss of different TezRs instigates significant alterations in gene expression and proteins synthesis.

Keywords: Receptors, Bacterial receptor, Chemotaxis, Extracellular DNA, Extracellular RNA, Nucleic-acids-based receptors, DNase, RNase, Teazeled receptors, TezR

Introduction

To ensure survival, bacteria need to adapt to a constantly changing environment. Despite the obvious significance of this process, many of its details have remained elusive [1–3]. At present, these adaptations are known to be mediated by a variety of predominantly transmembrane receptors consisting of a protein structure, which control different key aspects of the interaction with the environment, cell-to-cell signaling, and multicellular behavior. The most well-known is a two-component regulatory system that is a stimulus–response coupling mechanism that is comprised of a membrane-localized histidine sensor kinase, and a cytoplasmically localized response regulator allowing bacteria to sense and respond to changes of different environmental conditions [4]. In signal transduction, kinase senses a particular external stimulus, undergoes autophosphorylation and transfers a phosphate molecule to the response regulator, resulting in its conformation alterations that promote a change in target gene expression [5–8].

Chemoreceptors represent the most well studied type of bacterial receptors [3, 9–12]. They recognize various signals, primarily growth substrates or toxins [13, 14]. Chemoreception is tightly linked to chemotaxis and provides bacteria with the capacity to approach or escape different compounds, thus favoring the movement toward optimal ecological niches [15]. However, many aspects of chemoreception remain unclear, including details of the mechanisms underlying high sensitivity, sensing of multiple stimuli, and recognition of previously unknown nutrients or xenobiotics [16–18].

*Correspondence: g.tetz@hmi-us.com

Human Microbiology Institute, New York, NY 10013, USA

© The Author(s) 2022. **Open Access** This article is licensed under a Creative Commons Attribution 4.0 International License, which permits use, sharing, adaptation, distribution and reproduction in any medium or format, as long as you give appropriate credit to the original author(s) and the source, provide a link to the Creative Commons licence, and indicate if changes were made. The images or other third party material in this article are included in the article's Creative Commons licence, unless indicated otherwise in a credit line to the material. If material is not included in the article's Creative Commons licence and your intended use is not permitted by statutory regulation or exceeds the permitted use, you will need to obtain permission directly from the copyright holder. To view a copy of this licence, visit http://creativecommons.org/licenses/by/4.0/. The Creative Commons Public Domain Dedication waiver (http://creativecommons.org/publicdomain/zero/1.0/) applies to the data made available in this article, unless otherwise stated in a credit line to the data.

Bacterial receptive function and interaction with the environment is coupled to bacterial memory, another poorly characterized phenomenon [19–25].

Cell memory is viewed as a part of history-dependent behavior and is intended as a means for the efficient adaptation to recurring stimuli. It is believed to be encoded by membrane potential, which is also associated with transmembrane receptors in bacteria [26].

Sensing of physical factors by bacteria remains even more elusive. For example, the mechanism of magnetoreception, whereby microorganisms sense the geomagnetic field, has been well described only in magnetotactic bacteria [27]. These prokaryotes sense magnetic fields due to the biomineralization of nano-sized magnets, termed magnetosomes, within cells [28, 29]. However, existing studies have not explained why bacteria lacking these elements could still sense the magnetic field [30, 31]. Recent data suggest that intracellular DNA can be affected by magnetic fields and is able to interact with them, but the nature of such interactions remains enigmatic [32–34].

The mechanism and regulation of bacterial temperature sensing is also characterized by numerous unknowns. Different studies have pointed to Tar/Tsr receptors as responsible for controlling and regulating the temperature response, but the detailed mechanisms of their reception remain elusive [35–38]. Some authors also highlight the sensing of the temperature that is associated with blue-light sensing through the BlsA Sensor [39, 40].

Therefore, the question of how known receptors sense a diverse array of chemical, biological, and physical factors remains insufficiently explored. It has been suggested that certain protein receptors could be organized into sensory arrays, whereby cooperative interactions between receptors enable the sensing of a diverse range of stimuli [12, 41–44]. Still, even such clusters could not account for the totality of different stimuli sensed by bacteria. Even in the case of known receptive systems it remains to be determined how bacteria sense the whole plethora of available environmental factors including previously unknown exogenous stimuli, how remote sensing operates, what is the common sensor part of most receptors, and how signal transduction is mediated. Therefore, a better understanding of receptors and receptor systems could expand our knowledge of the regulation of bacterial physiology, virulence, and adaptation.

Here, we report for the first time the identification of a previously unknown universal system in bacteria that is responsible for the interaction of cells with the environment. We found that this system includes DNA- and RNA-based elements located outside the cell membrane, which form a cloudy network around the cells and perform receptive and regulatory functions. Due to their similarity with the spiny bracts of *Dipsacus* spp., we have named this cloudy network Teazeled (common name of *Dipsacus* spp.) receptors (TezRs) and the system, Teazeled receptor system (TR-system). The TR-system also includes transcriptases and recombinases. Recently, the identical TezRs were found on the surface of mammalian, fungal and plant cells [45].

Materials and methods

Bacterial and phage strains and culture conditions

Bacillus pumilus VT1200, *Staphylococcus aureus* MSSA VT209, *Staphylococcus aureus* SA58-1, *Pseudomonas putida* VT085, and *Escherichia coli* LE392 infected with bacteriophage λLZ1 [gpD-GFP b::ampR, kanR] bearing ampicillin and kanamycin resistance were obtained from a private collection (provided by Dr. V. Tetz). *Escherichia coli* ATCC 25922 was purchased from the American Type Culture Collection (Manassas, VA, USA). Bacterial strains were passaged weekly on Columbia agar (BD Biosciences, Franklin Lakes, NJ, USA) and stored at 4 °C. All subsequent liquid subcultures were derived from colonies isolated from these plates and were grown in Luria–Bertani (LB) broth (Oxoid, Hampshire, UK; Sigma-Aldrich, St Louis, MO, USA), Columbia broth (BD Biosciences) or nutrient broth (CM001; Oxoid), if not stated otherwise. Other liquid media included M9 Minimal Salts (Sigma-Aldrich). For experiments on sold media, bacteria were cultured on Columbia agar, nutrient agar (CM003; Oxoid), TGV agar (TGV-Dx, Human Microbiology Institute, New York, NY, USA), LB agar (Sigma-Aldrich), Aureus ChromoSelect Agar Base (Sigma-Aldrich), tryptic soy agar (Sigma-Aldrich), and egg-yolk agar (Hardy Diagnostics, Santa Maria, CA, USA). Sheep red blood cells were purchased from Innovative Research (Peary Court, MI, USA). All cultures were incubated aerobically at 37 °C in a Heracell 150i incubator (Thermo Scientific, Waltham, MA, USA) if not stated otherwise. For anaerobic growth experiments, *P. putida* VT085 was plated on agar and cultivated in AnaeroGen 2.5-L Sachets (Oxoid) placed inside a CO2 incubator (Sanyo, Kitanagoya, Aichi, Japan) at 37 °C for 24 h.

Reagents

Bovine pancreatic DNase I with a specific activity of 2200 Kunitz units/mg and RNase A (both Sigma-Aldrich), or human recombinant DNase I (Catalent, US) were used at concentrations ranging from 1 to 10 μg/ml. Ampicillin, kanamycin, rifampicin, vancomycin, nevirapine, etravirine, raltegravir, lactose, povidone iodine and dexamethasone were obtained from Sigma-Aldrich.

Removal of TezRs

To remove primary TezRs, bacteria were harvested by centrifugation at 4000 rpm for 15 min (Microfuge 20R; Beckman Coulter, La Brea, CA, USA), the pellet was washed twice in phosphate-buffered saline (PBS, pH 7.2) (Sigma-Aldrich) or nutrient medium to an optical density at 600 nm (OD600) of 0.003–0.5. Bacteria were treated for 30 min at 37 °C with nucleases (DNase I or RNase A), if not stated otherwise, washed three times in PBS or broth with centrifugation at 4000×*g* for 15 min after each wash, and resuspended in PBS or broth. Bacteria, whose TezRs were deactivated or made non-functional, were marked with the superscript letter "d". Control cells were processed in the same manner; however, instead of treatment with nucleases, they were treated with water (used as a vehicle for nucleases).To study secondary TezRs, 1.5% TGV agar was used. After autoclaving at 121 °C for 20 min, the agar was cooled down to 45 °C and DNase I or RNase A, or a mixture of the two, was added, mixed, and 20 mL of the solution was poured into 90-mm glass Petri dishes.

For biofilm formation assays, bacteria were separated from the extracellular matrix by washing three times in PBS or broth with centrifugation at 4000×*g* for 15 min after each wash. Then, 25 µL of suspension containing 7.5 log10 cells was inoculated into the center of the prepared solid medium surface supplemented or not with nucleases and incubated at 37 °C for different times.

Inactivation of TezRs with propidium iodine

To inactivate primary TezRs, bacteria were harvested by centrifugation at 4000 × g for 15 min (Microfuge 20R; Beckman Coulter, La Brea, CA, USA). The pellet was washed twice in PBS, pH 7.2 (Sigma-Aldrich). Bacteria were treated with propidium iodine (PI) for 30 min at 37 °C. If not stated otherwise, the PI-treated cells were washed three times in PBS with subsequent centrifugation at 4000×*g* for 15 min, and resuspended in PBS or nutrient medium.

Generation of anti-RNA and anti-DNA antibodies

For the isolation of extracellular DNA and RNA, 24 h old biofilms were *B. pumilus* grown on the agar were washed with PBS, centrifuges 4000×*g* for 15 min and supernatant was filtered through a 0.22 µm filter (Millipore Corp., Bedford, MA, USA). Extracellular RNA was extracted by using RNeasy Mini Kit (Qiagen, Valencia, CA) and extracellular DNA with DNeasy Mini Kit (Qiagen, Valencia, CA) according to the manufacturer's instructions. Antibodies against extracellular DNA and RNA were obtained after New Zealand White 4 months of age rabbit immunization with nucleic acids and a complete Freund's adjuvant according to Cold Spring Harbor protocol for standard immunization of rabbits [46].

Growth curve

For growth rate determination at the various time points, stationary phase bacteria were washed from the extracellular matrix, treated with nucleases (10 µg/mL), and 5.5 log10 cells were inoculated into 4.0 mL Columbia broth. OD600 was measured on a NanoDrop OneC spectrophotometer (Thermo Scientific).

Bacterial viability test

To evaluate bacterial viability, bacterial suspensions were serially diluted and 100 µL of the diluted suspension was spread onto agar plates. Plates were incubated at 37 °C overnight and colony forming units (CFU) were counted the next day.

Biofilm morphology

To culture bacterial biofilms, we prepared glass Petri dishes containing TGV agar supplemented or not with 10 µg/mL DNase I or RNase A, or a mixture of the two. Then, 25 µL of a suspension containing 5.5 log10 cells was inoculated in the center of the agar and the dishes were incubated at 37 °C for different times. The biofilms were photographed with a digital camera (Canon 6; Canon, Tokyo, Japan) and analyzed with Fiji/ImageJ software [47].

Fluorescence microscopy

Differential interference contrast (DIC) and fluorescence microscopy were used to confirm the destruction of primary TezRs with nucleases. Bacteria treated or not with nucleases were sampled at OD600 of 0.1, washed from the matrix, fixed in 4% paraformaldehyde/PBS (Sigma-Aldrich) for 15 min at room temperature, and stored at 4 °C until use. Bacteria were centrifuged at 14,000×*g* and cell pellets were dispersed in 10 µL PBS, incubated with SYTOX Green at a final concentration of 2 µM, and mounted in Fluomount mounting medium. Cells were imaged using an EVOS FL Auto Imaging System (Thermo Scientific) equipped with a 60× or 100× objective and 2× digital zoom.

Membrane-impermeable SYTOX Green stained cell surface-bound DNA and RNA. A reduction of green fluorescence compared to the untreated control, enabled the visualization of alterations elicited by nuclease treatment. Dead cells with permeable membranes showed a higher level of green fluorescence and were discarded from the analysis. No post-acquisition processing was performed; only minor adjustments of brightness and contrast were applied equally to all images. ImageJ software was used

to quantify the signal intensity per cell; at least five representative images (60 × field) were analyzed for each case [48].

Light microscopy-based methods

Samples were imaged on an Axios plus microscope (Carl Zeiss, Jena, Germany) equipped with an ApoPlan × 100/1.25 objective. Images were acquired using a Canon 6 digital camera. Cell size was determined by staining cell membranes with methylene blue or Gram staining (both Sigma-Aldrich) and quantification in Fiji/ImageJ software. Values were expressed in px2 [47].

Assays of RNase internalization

The internalization of RNase A was visualized in *B. pumilus*. *B. pumilus* (5.5 $\log_{10}$ cells/ml) in PBS were incubated with fluorescein isothiocyanate (FITC) labeled RNase A at 37 oC for 15 or 60 min as previously described [49]. Bacteria were washed three times with PBS to remove any unbound protein. After washing the bacteria is cultivated for 2 h in LB broth, washed to remove residual media components, and placed on a microscope slide for visualization. Fluorescence was monitored using a fluorescence microscope (Axio Imager Z1, Carl Zeiss, Germany). To visualize the internalization of RNase A, the biofilms of *B. pumilus* incubated with 100 µg/mL fluorescein-labeled RNase A were obtained as described earlier. After 24 h of growth at 37 °C, bacteria were washed three times with PBS to remove unbound proteins, and placed on a microscope to monitor the fluorescence using a fluorescence microscope (Axio Imager Z1, Carl Zeiss, Germany).

Generation of RNA sequencing data

To isolate RNA, the cell suspension obtained 2.5 h post-nuclease treatment were washed thrice in PBS,pH 7.2 (Sigma) and centrifuged each time at 4000×*g* for 15 min (Microfuge 20R, Beckman Coulter) followed by resuspension in PBS.

RNA was purified using RNeasy Mini Kit (Qiagen) according to the manufacturer's protocol. The quality of RNA was spectrophotometrically evaluated by measuring the UV absorbance at 230/260/280 nm with the NanoDrop OneC spectrophotometer (ThermoFisher Scientific).

Transcriptome sequencing (RNA-Seq) libraries were prepared using an Illumina TruSeq Stranded Total RNA Library Prep kit. RNA was ribodepleted using the Epicenter Ribo-Zero magnetic gold kit (catalog no. RZE1224) according to the manufacturer's guidelines. The libraries were pooled equimolarly and sequenced in an Illumina NextSeq 500 (Illumona, San Diego CA) platform with paired 150-nucleotide reads (130MM reads max).

Analysis of RNA sequencing data

Sequencing reads were mapped corresponding to the reference genome of *S. aureus* NCTC 8325 (NCBI Reference Sequence: NC–007795), and expression levels were estimated using Geneious 11.1.5. Transcripts with an adjusted P value of < 0.05 and $\log_2$ fold change value of ± 0.5 were considered for significant differential expression. PCA, volcano plots and Euclidean distances plots were generated using the ggplot2 package in R, and the Venn diagram was obtained using BioVenn [50].

Sporulation assay

Sporulation was analyzed under the microscope by counting cells and spores in 20 microscope fields and three replicates. For each image, we calculated the number of spores and the number of cells. Then, we plotted the ratio of spores to the combined number of cells and spores in each bin. Sporulation under stress conditions was carried out by heating the bacterial culture at 42 °C for 15 min.

Modulation of thermotolerance

Overnight *S. aureus* VT209 cultured in LB broth supplemented or not with raltegravir (5 µg/mL) was separated from the extracellular matrix by washing in PBS and then diluted with PBS to OD600 of 0.5. Bacteria were treated with nucleases to remove primary TezRs or were similarly treated with water and 5.5 log10 CFU/mL were placed in 2-mL microcentrifuge tubes (Axygen Scientific Inc., Union City, CA, USA). Each tube was heated to 37, 40, 45, 50, 55, 60, 65, 70 or 75 °C in a dry bath (LSETM Digital Dry Bath; Corning, Corning, NY, USA) for 15 min. After heating, control *S. aureus* were immediately treated with nucleases to delete primary TezRs, washed three times to remove nucleases, serially diluted, plated on LB agar, and the number of CFU was determined within 24 h.

Modulation of thermotolerance restoration after TezRs loss

To determine the time it took for thermotolerance to be restored in bacteria following TezRs removal, overnight *S. aureus* VT209 cultures were treated with 10 µg/mL DNase I or RNase A, or a mixture of the two. Bacteria lacking TezRs were inoculated in LB broth and sampled hourly for up to 8 h. The samples were heated at the maximum temperature tolerated by the bacteria and viability was assessed as described in the previous section. Untreated *S. aureus* were used as a control and were processed the same way by heating at the lowest

non-tolerable temperature, serially diluted, plated on LB agar, and assessed for CFUs within 24 h. Complete restoration of normal temperature tolerance coincided with growth inhibition at higher temperatures. The experiment was not extended beyond this time point.

Bacteriophage infection assay

An overnight *E. coli* LE392 culture was diluted 1:1000 and grown in liquid LB broth supplemented with 0.2% maltose and 10 mM MgSO4 at 30 °C for 18–24 h, until OD600 of 0.4. Cells were separated from the extracellular matrix by three washes in PBS and centrifugation at 4000×*g* for 15 min and 20 °C after each wash, followed by resuspension in ice-cold LB broth supplemented with 10 mM MgSO4 to OD600 of 1.0. Approximately 10 µL of plaque-forming units of the purified λ phage was added to 200 µL *E. coli* LE392 with intact TezRs. The suspension was incubated for 30 min on ice and another 90 min at room temperature to ensure that the phage genome entered the cells [51]. The remaining phages were removed by three washes in PBS and centrifugation at 4000×*g* for 15 min and 20 °C after each wash.

Bacteria were treated with nucleases to destroy primary TezRs, followed by three centrifugation steps at 4000×g for 15 min and 20 °C. Control *E. coli* were similarly treated with water. After that, 100 µL of bacterial suspension was plated as a lawn on LB agar supplemented with 10 µg/mL kanamycin and 100 µg/mL ampicillin, incubated for 24 h at 30 °C, and the number of Amp/Kanr colonies was determined.

Persister assay

E. coli ATCC 25,922 were treated with nucleases to remove primary TezRs, inoculated in LB broth supplemented with ampicillin (150 µg/mL), and incubated at 37 °C for 6 h. Samples taken before and after incubation with ampicillin were plated on LB agar without antibiotics to determine the CFU [52]. The frequency of persisters was calculated as the number of persisters in a sample relative to the number of cells before antibiotic treatment in each probe.

Analysis of virulence factors production

S. aureus SA58-1 were treated with nucleases to remove primary TezRs and resuspended in PBS to 6.0 log10 CFU/mL. The hemolytic test was performed as previously described with minor modifications [53]. Briefly, bacterial cells were plated in the center of Columbia agar plates supplemented with 5% sheep red blood cells and incubated at 37 °C for 24 h. A greenish zone around the colony denoted α-hemolysin activity; whereas β-hemolysin (positive) and γ-hemolysin (negative) activities were indicated by the presence or absence of a clear zone around the colonies. The size of the hemolysis zone (in mm) was measured.

Lecithinase activity by bacteria with intact TezRs or lacking TezRs was determined by plating cells on egg-yolk agar and incubation at 37 °C for 48 h. The presence of the precipitation zone and its diameter were evaluated [54].

UV assay

S. aureus VT209 were treated with nucleases to remove primary TezRs. Control probes were treated with water. Bacteria at 8.5 log10 CFU/mL in PBS were added to 9-cm Petri dishes, placed under a light holder equipped with a new 254-nm UV light tube (TUV 30 W/G30T8; Philips, Amsterdam, The Netherlands), and irradiated for different times at a distance of 50 cm. After treatment, bacteria were serially diluted, plated on nutrition agar plates, incubated for 24 h, and CFU were determined.

Animal models

All animal procedures and protocols were approved by the institutional animal care and use (IACUC) committee at the Human Microbiology Institute (protocol: # T-19-204) and all efforts were made to minimize animal discomfort and suffering. Adult C57BL/6 mice weighing from 18 to 20 g (Jackson Laboratories, Bar Harbor, ME, USA) were fed ad libitum and housed in individual cages in a facility free of known murine pathogens. Animals were cared for in accordance with National Research Council recommendations, and experiments were carried out in accordance with the Guide for the Care and Use of Laboratory Animals [55].

Animals were randomly designated to four groups of eight mice each, which were used to measure the load of *S. aureus* SA58-1. Mice were anesthetized with 2% isoflurane, and intraperitoneally injected with nuclease-treated *S. aureus* at 10.1 log10 to 10.2 log10 CFU/mouse. Control animals received *S. aureus* SA58-1 treated with water. After 12 h, mice were euthanized by CO2 and cervical dislocation, and the bacterial load in the peritoneum, liver, spleen, and kidneys was determined by serial dilution and CFU counts after 48 h of culture on plates with selective *S. aureus* agar. Cell morphology was determined under an Axios plus microscope, following staining with a Gram stain kit (Merck, Darmstadt, Germany).

Magnetic exposure conditions

The effect of the TRB-receptor system on regulation of *B. pumilus* VT1200 growth when exposed to regular magnetic and shielded geomagnetic fields was assessed. *B. pumilus* lacking primary and secondary TezRs were obtained as previously discussed. Final inoculi of 5.5

log10 CFU/mL in 25 µL were dropped in the center of agar-filled Petri dishes. Magnetic exposure conditions were modulated by placing the Petri dish in a custom-made box made of five layers of 10-µm-thick µ metal (to shield geomagnetic field) at 37 °C for 24 h. Biofilm surface coverage was analyzed using Fiji/ImageJ software and expressed as px2 [48, 56].

In a second experimental, *B. pumilus* VT1200 with intact TezRs and missing TezR–R1 were exposed to regular magnetic conditions or a shielded geomagnetic field as described above, and colony morphology was analyzed after 8 and 24 h. Images of the plates were acquired using a Canon 6 digital camera.

Estimation of spontaneous mutation rates

To calculate the number of mutation events, we used *E. coli* ATCC 25922, treated with nucleases to remove primary TezRs or untreated controls, and standardized at 9.0 log10 cells. The number of spontaneous mutations to RifR was used to estimate the mutation rate. This was determined by counting the number of colonies formed on Mueller–Hinton agar supplemented or not with rifampicin (100 µg/mL). After incubation at 37 °C for 48 h, CFU as well as rifampicin resistant mutants were counted and the mutation rate was calculated by the Jones median estimator method [57].

Light exposure experiments

B. pumilus VT1200 lacking primary and secondary TezRs were obtained as described previously. An aliquot containing 5.5 log10 bacteria in 25 µL was placed in the center of Columbia agar plates, which were then incubated at 37 °C for 7 or 24 h while irradiated with halogen lamps of 150 W (840 lm) (Philips, Shanghai, China). Colonies were photographed with a Canon 6 digital camera. The distance between the light source and the sample was 20 cm. Control probes were processed the same way, but were grown in the dark.

Chemotaxis and dispersal measurements

The assay was performed as described previously with some modifications. Briefly, 250 µL fresh human plasma filtered through a 0.22-µm pore-size filter (Millipore Corp., Bedford, MA, USA) immediately prior to use, was spread using a sterile L-shape cell spreader onto a sector comprising 1/6 of the plate of the 90 mm glass Petri dish filled with 1.5% TGV agar. *B. pumilus* VT1200 devoid of primary and secondary TezRs were obtained as described previously. An aliquot containing 5.5 log10 cells in 25 µL was placed in the center of the plates, which were then incubated at 37 °C for 24 h and photographed with a Canon 6 digital camera. Chemotaxis was evaluated by measuring the migration of the central colony towards the plate sector containing plasma. Colony dispersal was assessed based on the appearance of small colonies on the agar surface.

Written informed consent was obtained from all patients to use their blood samples for research purposes, and the study was approved by the institutional review board of the Human Microbiology Institute (# VB-021420).

Effect of reverse transcriptase inhibitors and integrase on bacterial growth

Minimum inhibitory concentrations (MICs) of nevirapine and etravirine against *S. aureus* VT209 were evaluated. *S. aureus* VT209 with intact or missing primary TezRs were obtained as described previously. Bacteria were incubated in LB broth supplemented or not with nevirapine (5 µg/mL) or etravirine (5 µg/mL). These values corresponded to > 1/100 their MICs. Growth was monitored by measuring OD600 during the first 6 h of incubation at 37 °C and recorded at hourly intervals on a NanoDrop OneC spectrophotometer.

Biochemical analysis

Biochemical tests were carried out using the colorimetric reagent cards GN (gram-negative) and BCL (gram-positive spore-forming bacilli) of the VITEK® 2 Compact 30 system (BioMérieux, Marcy l'Étoile, France) according to the manufacturer's instructions. The generated data were analyzed using VITEK® 2 software version 7.01, according to the manufacturer's instructions.

Recognition of lactose and dexamethasone

The role of the TR-receptor system in the recognition of lactose and dexamethasone was investigated with *E. coli* ATCC 25,922 and *B. pumilus* VT1200. Bacterial suspensions of control bacteria and those lacking primary TezRs were adjusted to a common CFU value and incubated in fresh M9 medium supplemented or not with 146 mM lactose or 127 mM dexamethasone.

The lag phase, representing the period between inoculation of bacteria and the start of biomass growth, was measured by monitoring OD600. The lag phase reflects the time required for the onset of nutrient utilization [58, 59].

Cell memory formation experiments

The onset of bacterial memory was defined as the time required for dexamethasone to start being consumed (time lag) in dexamethasone-naïve and dexamethasone-sentient *B. pumilus* VT1200 and *E. coli* ATCC 25922. To study the first exposure to dexamethasone, *B. pumilus* or *E. coli* with intact TezRs were incubated in fresh M9 medium supplemented or not with 127 mM

dexamethasone for 24 h. To study the second exposure to dexamethasone, bacteria were taken after 24 h of cultivation from the first exposure to dexamethasone and washed three times in PBS with centrifugation at 4000×*g* for 15 min and 20 °C after each wash. Bacteria were adjusted to a common OD600 and incubated again in fresh M9 medium supplemented with dexamethasone. During the first and second exposures to dexamethasone, samples were taken at hourly intervals for the first 6 h and OD600 was measured with a NanoDrop OneC spectrophotometer to determine the lag phase. The different time lag between the first and second exposures to dexamethasone represented the formation of memory [60].

Evaluation of the role of TezRs in memory formation

To study the role of TezR–R1 in remembering previous exposures to nutrients, we assessed the difference in the time required for dexamethasone-naïve and dexamethasone-sentient *E. coli* ATCC 25922 to sense and trigger dexamethasone utilization. The two *E. coli* cell types with intact TezRs were pretreated with 127 mM dexamethasone for 5, 10, 15 or 20 min. Next, bacteria were treated with RNase A to remove TezR–R1, and inoculated in fresh M9 medium supplemented with dexamethasone. The lag phase prior to dexamethasone consumption was determined by monitoring OD600 every hour.

Memory loss experiments

The role of TezRs in bacterial memory loss was studied by comparing the lag phase of dexamethasone-naïve and dexamethasone-sentient *B. pumilus* VT1200 with intact TezRs [19]. Bacteria were cultivated in M9 medium supplemented with 127 mM dexamethasone for 24 h, centrifuged at 4000×*g* for 15 min, and washed in M9 medium without dexamethasone. The cells then underwent repeated rounds of TezR–R1 removal and restoration, followed by growth in culture broth without dexamethasone. After 24 h of cultivation at 37 °C, bacteria were isolated from the medium, TezR–R1 were removed again, and bacteria were re-inoculated in fresh culture broth. In total, cultivation in broth followed by TezR–R1 removal was repeated three times. Samples were taken prior to every TezR–R1 removal step, bacteria were washed, inoculated in M9 broth supplemented with dexamethasone, and the time lag to dexamethasone consumption was assessed by monitoring OD600.

After the third set of cultivation in M9 broth, bacteria were centrifuged and inoculated in fresh M9 broth. They were then cultivated for 24 h, centrifuged, washed, and inoculated in M9 broth supplemented with dexamethasone to mimic a second contact with dexamethasone. The time lag to dexamethasone consumption was assessed by monitoring OD600. Bacteria from the control group were processed the same way, but without undergoing TezR–R1 removal.

Raltegravir in cell memory formation experiments

The MIC of raltegravir against *S. aureus* VT209 was evaluated. To determine the effect of raltegravir on bacterial memory, *B. pumilus* VT1200 were grown on fresh M9 medium supplemented or not with 127 mM dexamethasone, with or without additionally supplementation with raltegravir (5 μg/mL, a 100-times lower concentration than the MIC). The biochemical profile of cells was analyzed with a VITEK® 2.

To evaluate the maximal time required for raltegravir to affect dexamethasone utilization, *B. pumilus* VT1200 were grown in M9 broth supplemented with 127 mM dexamethasone, while raltegravir was added at 0 h, 15 min, 30 min, 1 h or 2 h. The samples were taken at hourly intervals for the first 6 h to measure OD600 and determine the lag phase.

Statistics

At least three biological replicates were performed for each experimental condition unless stated otherwise. Each data point was denoted by the mean value ± standard deviation (SD). A two-tailed *t*-test was performed for pairwise comparisons and $p \leq 0.05$ was considered significant. Bacterial quantification data were log10-transformed prior to analysis. Statistical analyses for the biofilm assays and hemolysin test were performed using Student's *t*-test. Data from animal and sporulation studies were calculated using a two-tailed Mann–Whitney U test. GraphPad Prism version 9 (GraphPad Software, San Diego, CA, USA) or Excel 10 (Microsoft, Redmond, WA, USA) were applied for statistical analysis and illustration.

Results

Confirmation of the presence cell surface-bound nucleic acids

First, we confirmed the presence cell surface-bound nucleic acids based TezRs by studying the changes in fluorescence of washed planktonic *B. pumilus* VT1200 following their treatment with 10 μg/mL DNase I and RNase A for 15 min or a combination of the two. SYTOX Green-stained *B. pumilus* displayed clear green fluorescence, confirming the presence of cell surface-bound nucleic acids, which were not removed upon washing of culture medium or matrix (Fig. 1A, B).

Bacteria treated with either DNase or RNase alone exhibited a decrease, but not the total disappearance of fluorescence compared to control cells ($p < 0.0001$). Instead, bacteria treated with a combination of DNase and RNase revealed the total disappearance of surface fluorescence compared to single-nuclease treatment ($p < 0.0001$).

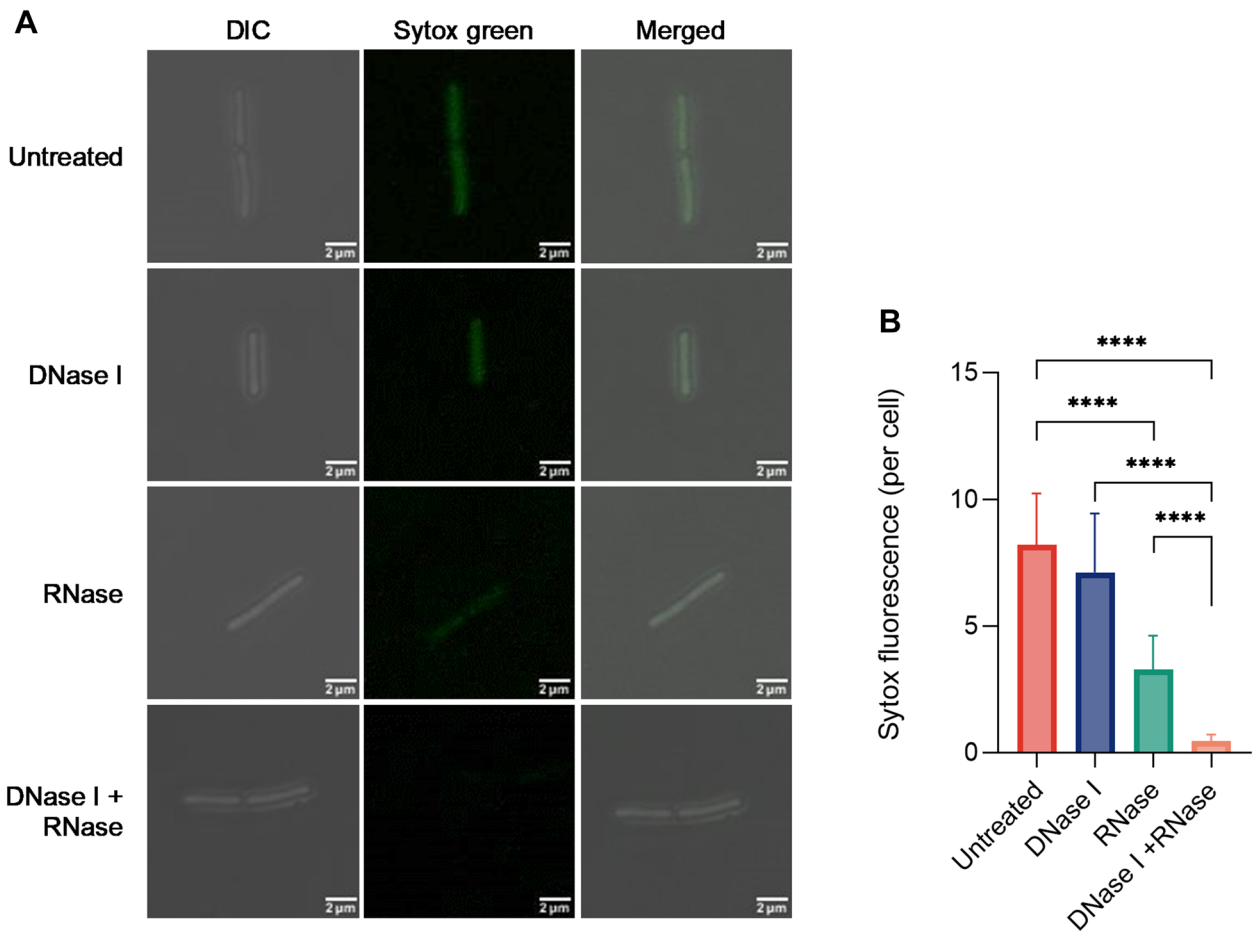

Fig. 1 Removal of *B. pumilus* cell surface-bound DNA and RNA molecules with nucleases. Green fluorescence denotes cell surface-bound DNA and RNA of *B. pumilus* stained with the membrane impermeable SYTOX Green dye. **A** DIC (left), SYTOX Green (center), and merged (right) images of control and DNase/RNase-treated *B. pumilus* at 100 × magnification. Scale bars represent 2 µm. **B** Quantification of SYTOX Green signal intensity per cell (n = 10; mean ± SD). ****p < 0.0001, two-tailed unpaired *t*-tests

Next, we verified that the RNase A used in this study was not internalized by the bacteria. To examine the ability of RNase A to penetrate the bacterial cell wall we linked the enzyme with a fluorophore. To score the penetration capability of RNase in *B. pumilus* we incubated *B. pumilus* on agar media supplemented with fluorophore-linked RNase or cultivated pre-treated *B. pumilus* with the same RNase. However, in both experiments no signs of RNase internalization were observed (Additional file 6: Fig. S1).

Classification and nomenclature of TezRs

We classified TezRs based on the structural features of their DNA- or RNA-containing domains, as well as association with the bacterial cell surface determined by the possibility of being washed into culture medium or matrix (Table 1).

To describe bacteria with certain deactivated TezRs, we marked them with the superscript letter "^{d}" (meaning deactivated).

As an example, *Escherichia coli* with deactivated primary DNA-formed TezR will be designated as "*E. coli* TezR-D1^{d}", where TezR stands for the receptor, followed by a dash, a capital letter representing the type of nucleic acid (D for DNA), an Arabic numeral representing the primary receptor, and "^{d}" indicating the deactivated status of this receptor. The same principle of naming is applicable for bacteria with other destroyed TezRs. Cells with multiple cycles of TezR destruction and restoration are named "zero cells" and are designated as "^{zdr}".

TezRs destruction has a global impact on gene expression

To gain insight into the consequences of TezRs loss on bacterial gene expression, RNA-seq analyses of *S. aureus* gene expression profile were examined following the

Table 1 Classification of TezRs in bacteria

Name of the receptor	Description of the receptor
Primary TezRs	
TezR–D1	DNA-based receptors located outside the membrane; they participate in cell regulation and are stably associated with the cell surface
TezR–R1	RNA-based receptors located outside the membrane; they participate in cell regulation and are stably associated with the cell surface
Secondary TezRs	
TezR–D2	DNA-based receptors located outside the membrane; they participate in cell regulation and can be easily washed out along with culture medium or matrix
TezR–R2	RNA-based receptors located outside the membrane; they participate in cell regulation and can be easily washed out along with culture medium or matrix

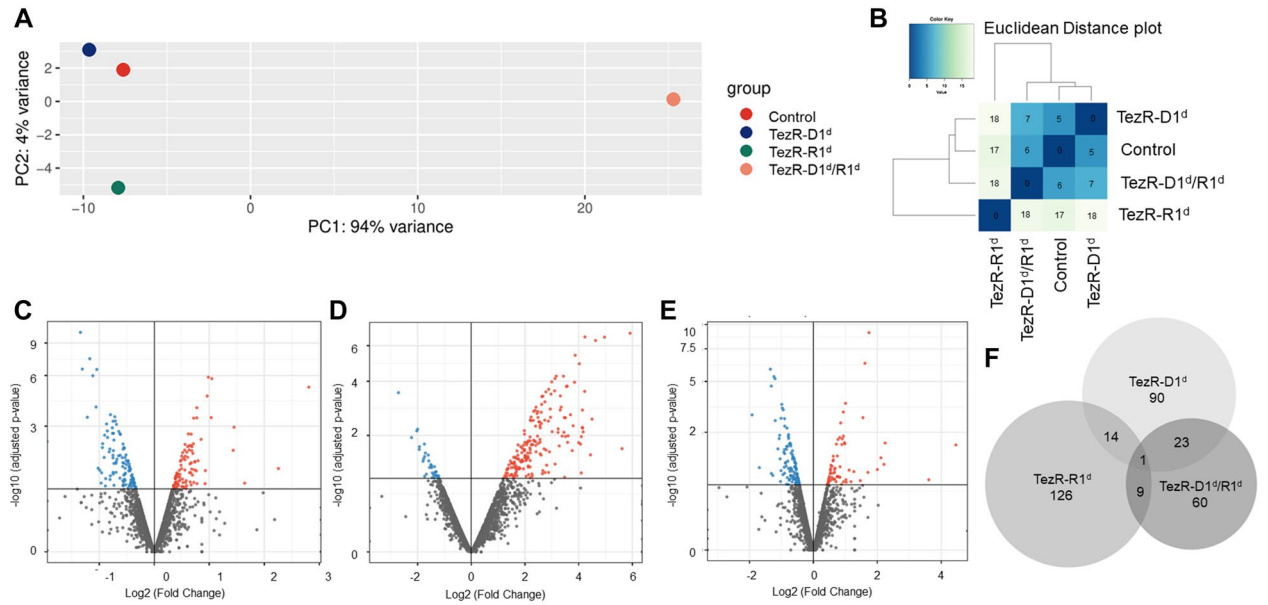

Fig. 2 Transcriptome analysis of *S. aureus* following the removal of primary TezRs. **A** PCA plot **B** Heatmap of Euclidean distance **C**–**E** Volcano plots highlighting the genes that are differentially expressed ($\log_2$ fold > 0.5 change plotted against the $-\log_{10}$ P-value). The results demonstrate the altered expression levels of the genes following primary TezRs loss (**F**) the overlap and unique DEPs in each group using Venn diagram

removal of primary TezRs. Principal-component analysis (PCA) showed that *S. aureus* due to the loss of primary TezRs clustered separately from the control group of *S. aureus* where TezRs was intact. The largest difference in PCA was observed for *S. aureus* TezR–$R1^d$ (Fig. 2A). These differences in gene expression datasets are also clearly evident in the hierarchical clustering and heatmaps of Euclidean distance. Strikingly, the largest pairwise Euclidean distance was observed between the control *S. aureus* and TezR–$R1^d$ (Fig. 2B).

Next, we compared the results from each probe and analyzed the genes whose expressions were significantly altered (upregulated or downregulated) following the removal of different TezRs (Fig. 2C–D). We identified 128, 150, and 93 differentially expressed proteins (DEPs) in *S.aureus* when compared to TezR–$D1^d$/control, TezR–$R1^d$/control, and TezR–$D1^d/R1^d$/control, respectively ($|\log_2$-fold change$| > 0.5$ and p-value < 0.05). Among the DEPs, 55 proteins were upregulated, and 73 proteins were downregulated in *S.aureus* TezR–$D1^d$ compared to those in the control (Fig. 2C). Among the DEPs in *S.aureus* TezR–$R1^d$, 137 upregulated and 13 downregulated proteins are found compared to those in the control (Fig. 2D). Additionally, 62 upregulated proteins and 31 downregulated proteins are detected in TezR–$D1^d/R1^d$ compared to those in the control. A minute overlap in differentially expressed transcripts were detected in bacteria after the removal of different TezRs. This non-redundancy signifies the individual regulatory roles of TezRs. These data evidently highlight the complex responses triggered by the loss of both primary DNA- and RNA-based TezRs, which cannot be justified by summing up

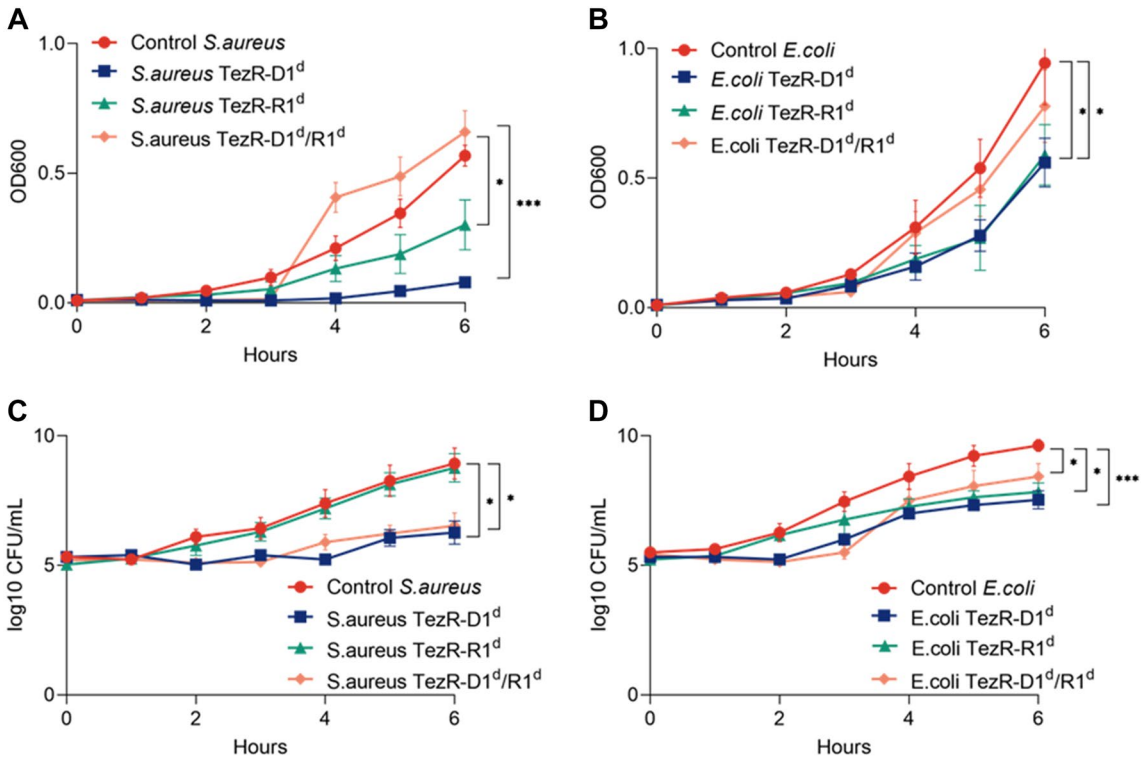

Fig. 3 Effect of TezR destruction on bacterial growth. Growth comparison of control bacteria and bacteria lacking TezR–D1 (*S. aureus* TezR–D1^d, *E. coli* TezR–D1^d), TezR–R1 (*S. aureus* TezR–R1^d, *E. coli* TezR–R1^d) or TezR–D1 and TezR–R1 (*S. aureus* TezR– TezR–D1^d/R1^d, *E. coli* TezR–TezR–D1^d/R1^d). (A, B) Bacterial growth measured as OD600 over time in (A) *S. aureus* and (B) *E. coli*. (C, D) Bacterial growth measured as bacterial counts (log10 CFU/mL) in (C) *S. aureus* and (D) *E. coli*. Values representing the mean ± SD were normalized to the initial OD600 value. *$p < 0.05$, ***$p < 0.001$

the effects of individual TezRs losses (Fig. 2E). The only gene expression which significantly altered due to the loss of any of the primary TezRs was SA0532 encoding a *Staphylococcus*-specific hypothetical protein [61]. Interestingly, following the loss of DNA-based TezRs alone or in combination with RNA-based TezRs, upregulation of proteins associated with type VII secretion system was observed [62, 63].

TezRs control microbial growth

Stationary phase *S. aureus* VT209 and *E. coli* ATCC 25922 were treated with water or pretreated with nucleases to remove primary TezRs, after which they were diluted in fresh medium and allowed to grow. OD600 and CFU were measured hourly during the first 6 h of incubation. Growth curves are presented as OD600 values (Fig. 3A, B) or bacterial counts (Fig. 3C, D) as a function of time.

Removal of primary TezRs retarded bacterial growth in both *S. aureus* and *E. coli* compared with control bacteria as measured by OD600 ($p < 0.001$ and $p < 0.05$, respectively) and CFU. While the lag phase was 3-h longer for treated *S. aureus*, it was similar between control and treated *E. coli*; although the latter exhibited retarded growth by the end of the observation period. At that point, CFU/mL of *S. aureus* TezR–D1^d and *E. coli* TezR–D1^d were lower by 2.6 log10 ($p < 0.05$) and 2.1 log10 ($p < 0.001$) compared with control bacteria.

Loss of TezR–R1 in *S. aureus* inhibited bacterial growth, as indicated by OD600 values ($p < 0.05$), but it did not affect bacterial counts. Such a discrepancy points to dysregulation of *S. aureus* TezR–R1^d and can be explained by reduced production of extracellular matrix. A similar effect on growth was observed in *E. coli* following the removal of TezR–R1 (OD600, $p < 0.05$); however, unlike in *S. aureus*, it coincided with reduced CFU ($p < 0.05$).

Loss of both primary TezRs in *S. aureus* and *E. coli* extended the lag phase by 3 h; however, this was followed by very rapid growth from 3 to 6 h. Thus, by the end of the observation period, OD600 for *S. aureus* TezR–D1^d/

R1^{d} was even higher than for control *S. aureus*; while OD600 for *E. coli* TezR–D1^{d}/R1^{d} was only marginally lower than for control *E. coli*. Surprisingly, bacterial counts of *S. aureus* TezR–D1^{d}/R1^{d} and *E. coli* TezR–D1^{d}/R1^{d} were lower throughout the observation period, amounting to 2.4 log10 CFU/mL and 1.2 log10 CFU/mL fewer counts compared with control bacteria after 6 h ($p < 0.05$). Cell size was also reduced at this time point (Additional file 1: Table S1).

The discrepancy between elevated OD600 levels along with delayed bacterial growth and a reduced cell size can be explained by the production of more extracellular matrix. Given similar OD600 values at the end of the observation period between control bacteria and those lacking TezR–D1/R1, we named the latter "Drunk cells".

Based on these and data we conclude that primary TezRs are required for the initial growth on the nutrient media and their destruction have individual consequences for cells.

Biofilm growth and cell size depend on TezRs

We next investigated how TezRs affected biofilm morphology of *B. pumilus* VT1200 grown on agar plates. To analyze the role of primary TezRs, *B. pumilus* were pretreated with nucleases and then inoculated and grown on regular agar medium. To study the role of secondary TezRs, growth of *B. pumilus* was evaluated on medium supplemented with different nucleases. We also established that RNase A used in this study was not internalized by the bacteria under these experimental conditions (Additional file 6: Fig. S1).

Loss of different TezRs resulted in changes to growth kinetics, biofilm formation, and cell size. The most significant alterations were noted for biofilms formed by motile bacteria lacking TezR–D2. These biofilms were characterized by formation of dendritic-like colony patterns, typical of cells with an increased swarming motility.

Biofilms of control *B. pumilus* had a circular shape (Fig. 4A) with smooth margins; whereas those formed by *B. pumilus* TezR–D1^{d} (Fig. 4B) and *B. pumilus* TezR–R1^{d} (Fig. 4C) develop blebbing, and those of *B. pumilus* TezR–D1^{d}/R1^{d} exhibited filamentous (filiform) margins (Fig. 4D).

B. pumilus TezR–D2^{d} biofilms were characterized by increased swarming motility and formation of significantly larger colonies ($p < 0.001$) with distinct phenotype and dendritic patterns (Fig. 4E); whereas *B. pumilus* TezR–R2^{d} biofilms had the same size as control *B. pumilus*, but irregular margins and wrinkled surface (Fig. 4F, Additional file 2: Table S2).

Interestingly, the combined removal of other TezRs along with loss of TezR–D2 led to a striking difference compared to the large biofilms formed by *B. pumilus* TezR–D2^{d}. The biofilms of both *B. pumilus* TezR–D2^{d}/R2^{d} and TezR–D1^{d}/R1^{d} were characterized by a structurally complex, densely branched morphology, but the dendrites were not so profound and the biofilm was not so spread out as in the case of *B. pumilus* TezR–D2^{d}. The morphology of biofilms formed by bacteria devoid of both primary and secondary TezRs such as *B. pumilus* TezR–D1^{d}/R1^{d}/D2^{d}/R2^{d} was very similar to that of *B. pumilus* TezR–D1^{d}/R1^{d}, with filamentous (filiform) margins but similar size as control *B. pumilus*.

In these experiments, nucleases added to the solid nutrient medium with the aim of removing secondary TezRs could potentially affect also cell surface-bound primary TezRs. However, a comparison of the morphology of biofilms formed by *B. pumilus* TezR–D1^{d} with those of *B. pumilus* TezR–D2^{d} and *B. pumilus* TezR–D1^{d}/D2^{d} (Fig. 4B, E, H) revealed clear differences, meaning that nucleases added to the agar did not alter primary TezRs, at least not in the same way as direct nuclease treatment did.

Moreover, the different size of biofilms formed by *B. pumilus* TezR–D2^{d} vs. *B. pumilus* TezR–D1^{d}/D2^{d} excludes the possibility that the increased colony size of the former resulted from greater swarming motility due to loss of extracellular DNA and decreased extracellular polysaccharide viscosity, because extracellular DNA was eliminated also in the latter [64]. Collectively, these data allow us to conclude that different TezRs play an individual role in biofilm morphology.

Next, we found that loss of TezRs had divergent effects on bacterial size. The combined removal of primary TezRs, or secondary TezR–D2 alone or in combination with other TezRs, resulted in significantly increased cell sizes ($p < 0.001$). In comparison, individual loss of secondary TezR–R2 decreased the size of *B. pumilus* cells ($p < 0.05$). Further experiments could not confirm an association between cell size alteration and sporulation

(See figure on next page.)

Fig. 4 TezRs regulate biofilm morphology and cell size. Morphology of nuclease-treated or control 72-h-old biofilms. (A) Control *B. pumilus*. (B) *B. pumilus* TezR–D1^{d}. (C) *B. pumilus* TezR–R1^{d}. (D) *B. pumilus* TezR–D1^{d}/R1^{d}. (E) *B. pumilus* TezR–D2^{d}. (F) *B. pumilus* TezR–R2^{d}. (G) *B. pumilus* TezR–D2^{d}/R2^{d}. (H) *B. pumilus* TezR–D1^{d}/D2^{d}. (I) *B. pumilus* TezR–D1^{d}/R1^{d}/D2^{d}/R2^{d}. Scale bars indicate 5 or 10 mm. Representative images of three independent experiments are shown. (J). Cell length of bacteria grown on solid medium (μm). *$p < 0.05$, ***$p < 0.001$. Data represent the mean ± SD from three independent experiments

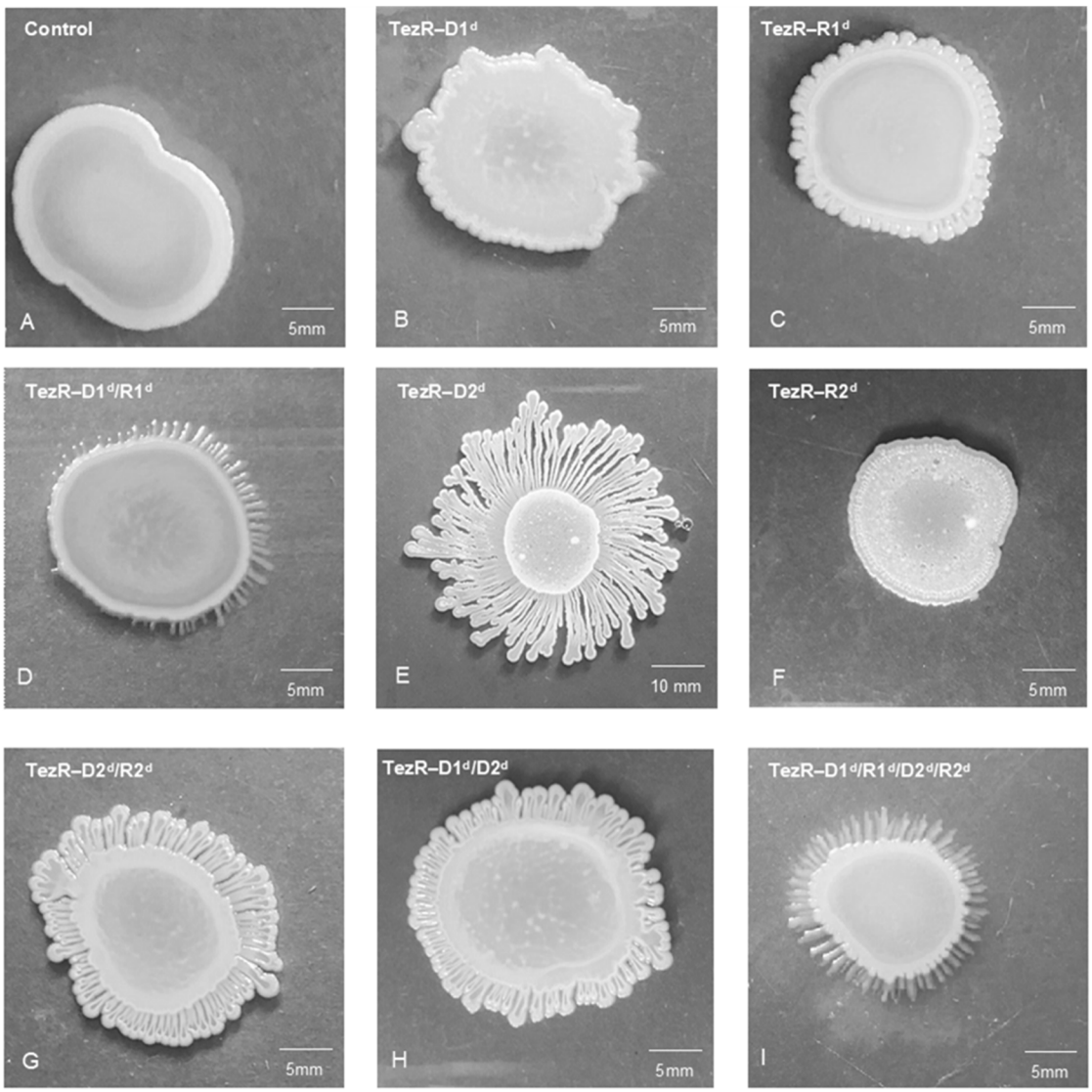

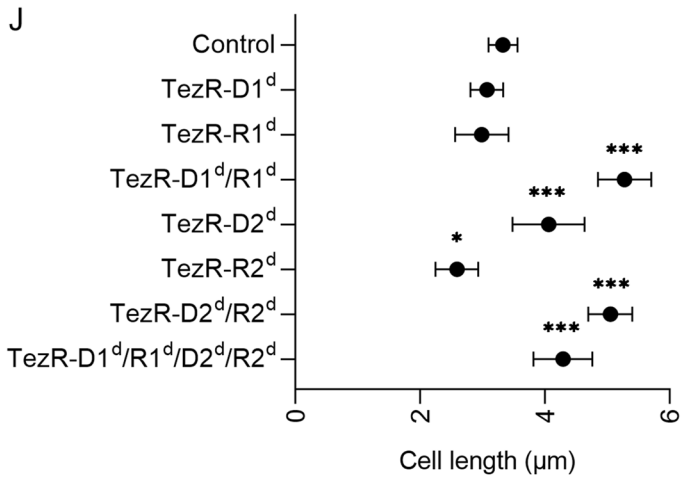

Fig. 4 (See legend on previous page.)

triggered by TezRs removal. Possibly, the observed greater mean cell length could result from incomplete cell division and elongation triggered by TezRs destruction [65].

Effect of TezR loss on sporulation

Given the significant alterations of biofilm morphology and transcriptome following TezRs loss, we sought evidence for their biological relevance in sporulation. We found that loss of TezR–D1, TezR–R1, and particularly TezR–R2 activated sporulation of *B. pumilus* VT1200 (all $p < 0.001$) (Fig. 5, Additional file 3: Table S3). In contrast, the inactivation of TezR–D2 completely repressed sporulation ($p = 0.007$) (Additional file 3: Table S3).

Heat map of sporulation intensity in cells with altered TezRs under normal conditions. Each cell indicates control *B. pumilus* or *B. pumilus* lacking TezRs. Color-coding indicates the ratio of spores to the total number of cells: white (0% sporulation), dark blue (100% sporulation).

Notably, sporulation was not affected in "Drunk cells" lacking TezR–D1/R1, but was increased if either TezR–D1 or TezR–R1 were removed. This finding highlights the complex web of pathways dictating the responses of "Drunk cells", which do not simply reflect the additive effect of removing individual primary TezRs. Moreover, the result points to the various roles of TezRs in controlling bacterial sporulation.

Role of TezRs in the regulation of stress responses

We next tested whether TezRs regulated also stress responses. The general stress response of control *B. pumilus* VT1200 manifested as increased sporulation (Fig. 6). Removal of TezR–R1 or TezR–R2 alone, or in combination with any other TezRs, upregulated the stress response and stimulated sporulation. Interestingly though, loss of TezR–D1 or TezR–D2 had the opposite effect ($p < 0.001$) (Additional file 4: Table S4). Hence, loss of TezR–D2 inhibited sporulation under both normal and stress conditions, confirming its implication in regulating the cell stress response.

Heat map of sporulation intensity in *B. pumilus* with altered TezRs under stress conditions. Each cell indicates control *B. pumilus* or *B. pumilus* lacking TezRs under stress conditions. Color-coding indicates the ratio of spores to the total number of cells: white (0% sporulation), dark blue (100% sporulation).

Dependence of temperature tolerance on TezRs

Assessment of whether bacterial thermotolerance depends of TezRs revealed that control *S. aureus* VT209 exhibited maximum tolerance at up to 50 °C, whereas *S. aureus* lacking primary TezRs could survive at even higher temperatures. Specifically, *S. aureus* TezR–D1^{d}

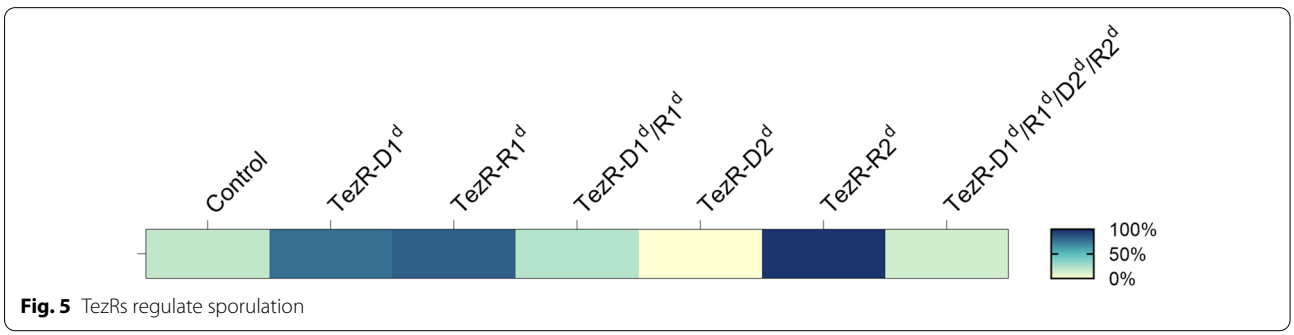

Fig. 5 TezRs regulate sporulation

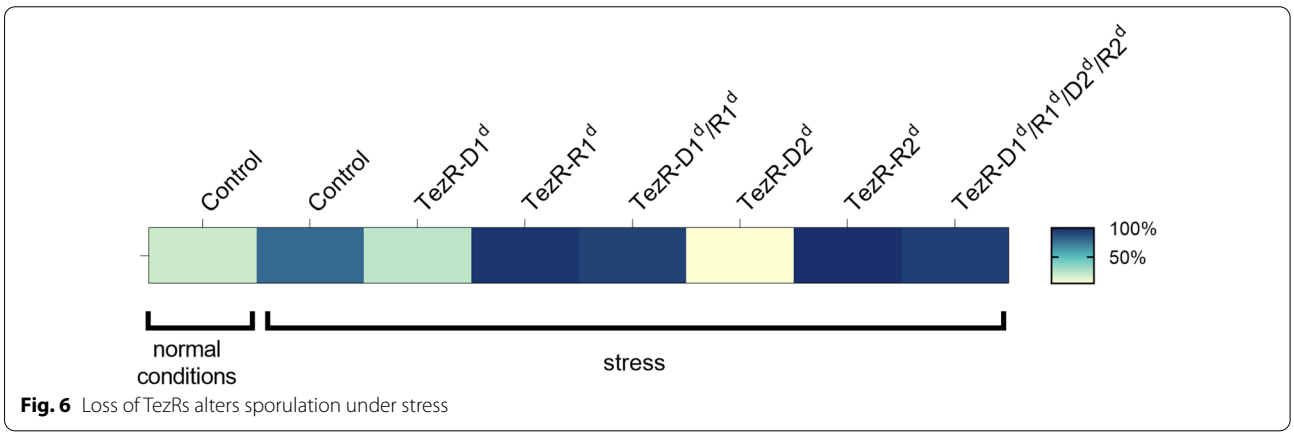

Fig. 6 Loss of TezRs alters sporulation under stress

survived at up to 65 °C, *S. aureus* TezR–R1^{d} at up to 70 °C, and *S. aureus* TezR–D1^{d}/R1^{d} at up to 60 °C (Fig. 7A).

We sought to discern whether the observed enhanced temperature survival was attributable to transcriptome-level responses triggered by TezRs removal, or to the direct role of TezRs in sensing and regulation of temperature changes. To this end, we incubated control *S. aureus* at different temperatures and removed primary TezRs right after heating to trigger transcriptionally-induced alterations. Loss of primary TezRs after the heating step did not improve temperature tolerance (Fig. 7B). This result demonstrated that the response of bacteria to higher temperatures was regulated by primary TezRs and depended on their presence at the time of heating, rather than being induced by their loss.

Next, we evaluated how much time was required for bacteria, which became resistant to heating after primary TezRs removal, to recover normal temperature sensing. This information could be used as a surrogate marker of the time required for restoration of functionally active cell surface-bound TezRs. *S. aureus* TezR–D1^{d}, TezR–R1^{d}, and TezR–D1^{d}/R1^{d} were inoculated in culture broth and grown at the maximum temperature tolerated by bacteria following each specific TezR destruction (65, 70, and 60 °C, respectively) (Fig. 7C). Control *S. aureus* were processed in the same way and heated at 55 °C as their next-to-lowest non-tolerable temperature. Each hour after heating, bacteria were inoculated in fresh LB broth to assess the presence or absence of growth after 24 h at 37 °C. Growth meant that bacteria still possessed enhanced temperature survival and the corresponding time indicated no restoration of functionally active primary TezRs. In turn, absence of growth could mean that functionally active primary TezRs were restored and bacteria could normally sense and respond to the higher temperature. After TezRs removal, it took from 7 to 8 h for *S. aureus* to restore functionally active primary TezRs and normal temperature tolerance (Fig. 7C). Taken together, these data demonstrate that TezRs participate in temperature sensing and the regulation of the corresponding response.

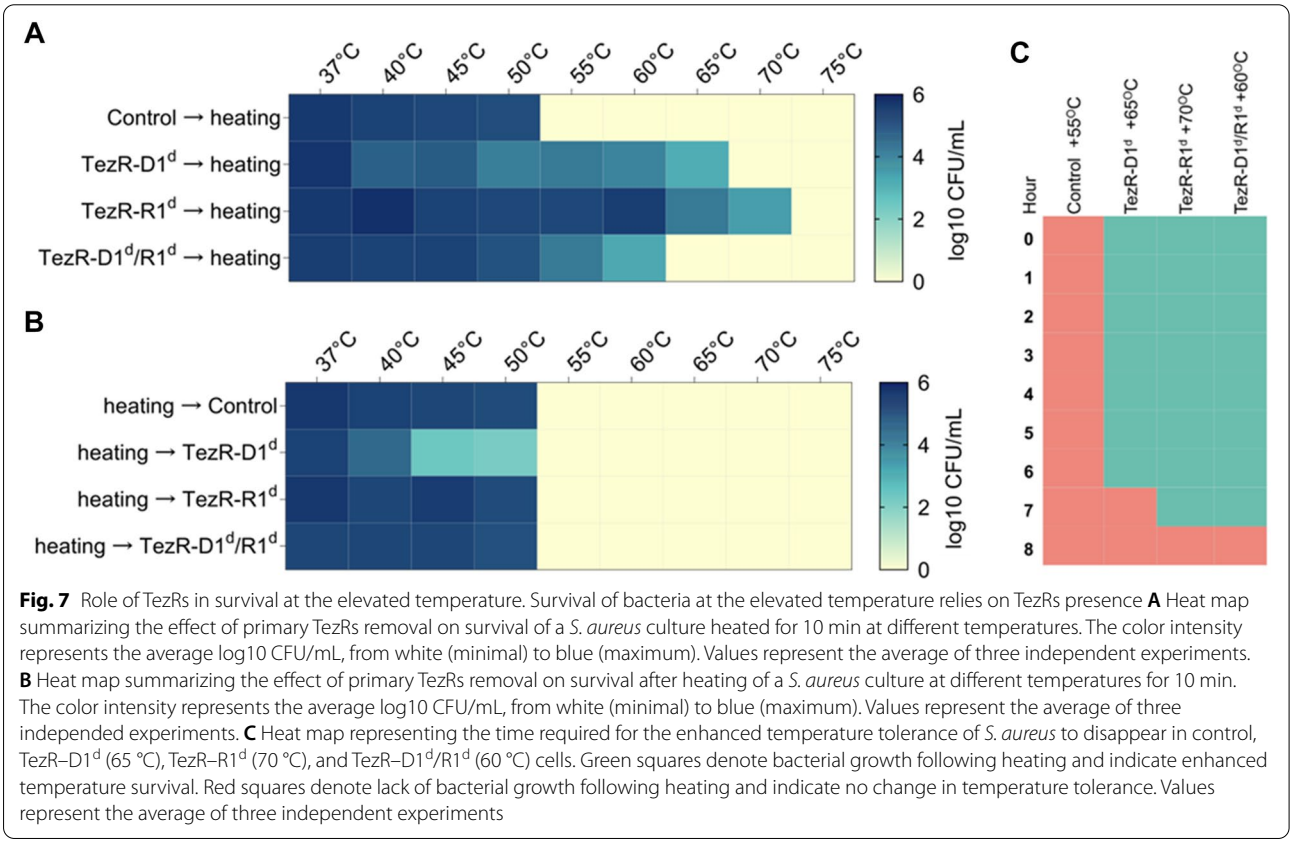

Fig. 7 Role of TezRs in survival at the elevated temperature. Survival of bacteria at the elevated temperature relies on TezRs presence **A** Heat map summarizing the effect of primary TezRs removal on survival of a *S. aureus* culture heated for 10 min at different temperatures. The color intensity represents the average log10 CFU/mL, from white (minimal) to blue (maximum). Values represent the average of three independent experiments. **B** Heat map summarizing the effect of primary TezRs removal on survival after heating of a *S. aureus* culture at different temperatures for 10 min. The color intensity represents the average log10 CFU/mL, from white (minimal) to blue (maximum). Values represent the average of three independed experiments. **C** Heat map representing the time required for the enhanced temperature tolerance of *S. aureus* to disappear in control, TezR–D1^{d} (65 °C), TezR–R1^{d} (70 °C), and TezR–D1^{d}/R1^{d} (60 °C) cells. Green squares denote bacterial growth following heating and indicate enhanced temperature survival. Red squares denote lack of bacterial growth following heating and indicate no change in temperature tolerance. Values represent the average of three independent experiments

TR-system manages resistance to UV

To determine whether TezRs participated in UV resistance, we exposed cells to UV light. Loss of TezR–D1 and TezR–D1/R1 had no statistically significant effect on the survival of *S. aureus* following UV irradiation compared to control bacteria (Fig. 8). Notably, loss of TezR–R1 protected bacteria from UV-induced death, and resulted in 2.4 log10 CFU/mL higher viable counts compared to control *S. aureus* following UV irradiation ($p = 0.002$). These data suggest that TezRs participate in sensing and response to UV irradiation.

Comparison of live bacteria measured as bacterial counts (log10 CFU/mL) before and after UV exposure. Data represent the mean ± SD of three independent experiments. $p < 0.05$ was considered significant.

Magnetoreception relies on TezRs

The magnetoreceptive function of TezRs was assessed by morphological changes at a macroscopic scale in agar-grown *B. pumilus* VT1200 biofilms following inhibition of the geomagnetic field (Fig. 9A, B).

Inhibition of the geomagnetic field promoted growth of control *B. pumilus* biofilms compared to cells grown under unaltered magnetic conditions (Fig. 9B–E). Loss of TezR–D1 or TezR–D2 stimulated bacterial growth in response to inhibition of the geomagnetic field across the entire plate (Fig. 9A). Instead, biofilms formed by *B. pumilus* following loss of TezR–R1 or TezR–R2 presented a strikingly diminished response to inhibition of the geomagnetic field. When compared with biofilms formed by control *B. pumilus*, those formed by *B. pumilus* TezR–R1^{d} or TezR–R2^{d} grown in a μ-metal cylinder for 24 h displayed only a negligible increase in size (Fig. 9A). However, they still exhibited minor changes in morphology compared with their counterparts grown under unaltered magnetic conditions (Fig. 9C, G).

To further elucidate the detailed role of RNA-based TezRs in sensing and responding to the geomagnetic field, we analyzed the time it took for morphological differences between control and *B. pumilus* TezR–R2^{d} biofilms placed in a μ-metal cylinder to occur. We found that already after 8 h, biofilms of control *B. pumilus* cultivated under inhibited geomagnetic field (Fig. 9D) presented an altered morphology with an increased size and irregular edge compared with those grown under normal conditions (Fig. 9B). In contrast, the morphology of *B. pumilus* TezR–R2^{d} biofilms was identical in the absence (Fig. 9F) or presence (Fig. 9B) of a regular geomagnetic field. These results showed that the alterations of biofilm morphology observed in *B. pumilus* TezR–R2^{d} in the inhibited geomagnetic field (Fig. 9G) occurred within 8–24 h. Together with our data pointing to the need for *S. aureus* for 8 h to restore normal temperature tolerance, these results add another line of evidence that bacteria started responding to geomagnetic field only after TezRs have been restored. Overall, RNA-based TezRs might be implicated in sensing the geomagnetic field and regulating cell responses to it. These findings also highlight the complex web of interactions between different TezRs, as some of them adapt their regulatory role to the presence or absence of other TezRs.

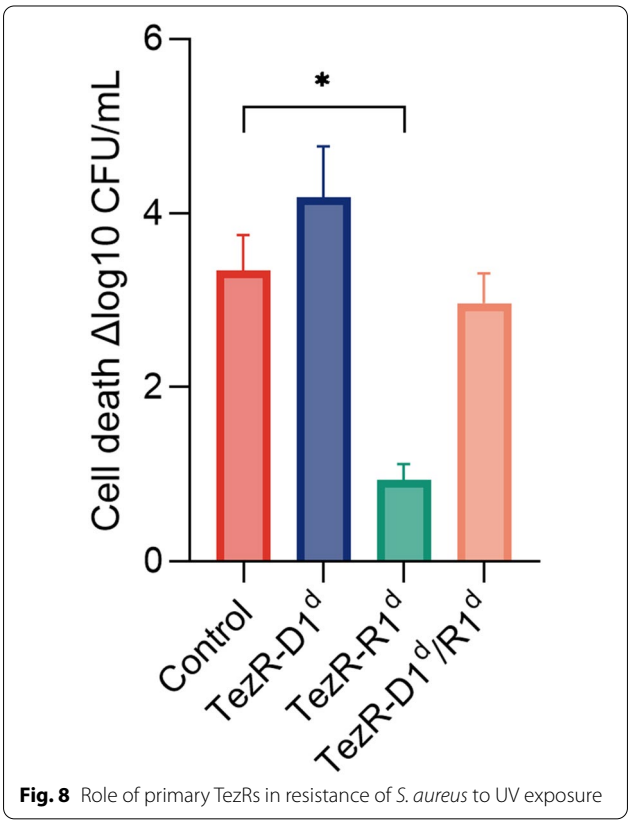

Fig. 8 Role of primary TezRs in resistance of *S. aureus* to UV exposure

TezRs are required by bacteria for light sensing

Given the broad functions of TezRs in mediating the interaction between bacteria and the surrounding environment, we sought evidence for their biological relevance in response to visible light. We analyzed differences in morphology of biofilms formed by control *B. pumilus* and *B. pumilus* following TezRs removal grown under light vs. dark conditions. Bacterial biofilms formed by either control *B. pumilus* or those lacking TezRs, except TezR–D2, responded to light by forming large biofilms with filamentous (filiform) margins (Fig. 10, Additional file 7: Fig. S2).

In contrast, *B. pumilus* TezR–D2^{d} grown under light exhibited reduced biofilm size compared to those grown under dark conditions (Additional file 7: Fig. S2). Strikingly, 24-h-old biofilms formed by *B. pumilus* TezR–R1^{d}

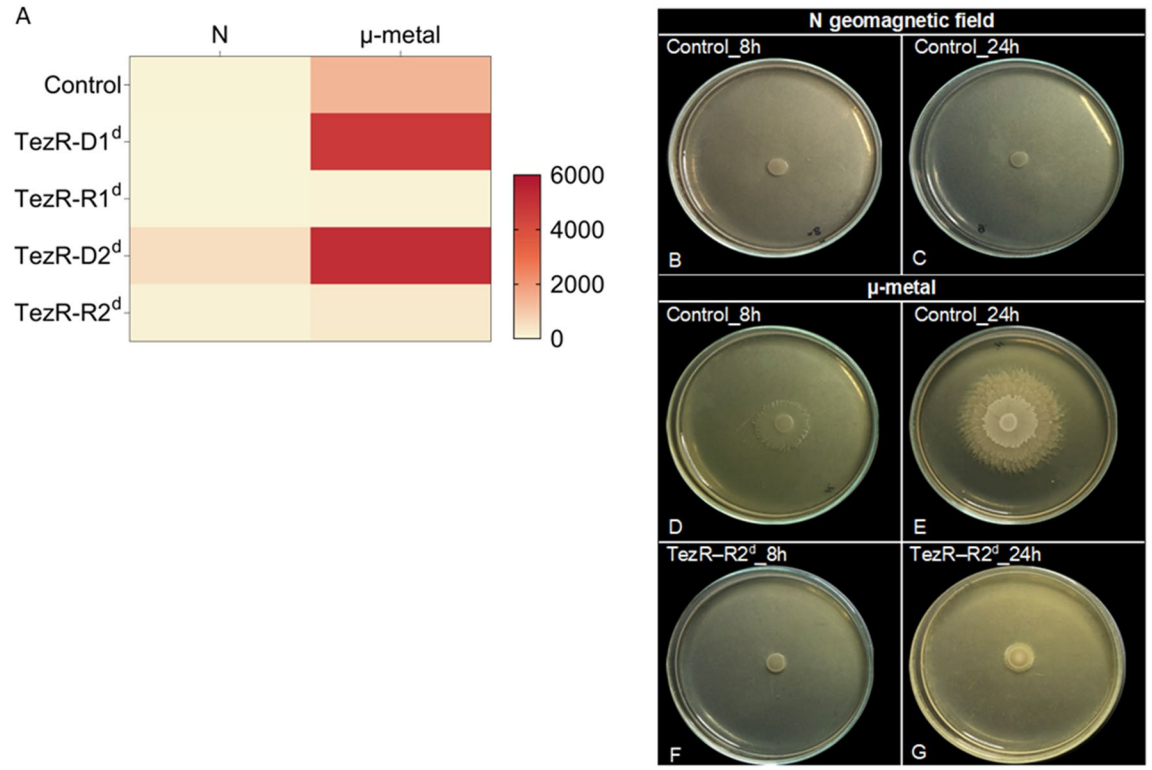

Fig. 9 Role of TezRs in magnetoreception of *B. pumilus*. **A** Heat map representing the effect of TezRs loss on the size of the biofilm area under normal (N) and inhibited geomagnetic (μ-metal) fields after 24 h of growth. The size of the biofilm is represented by a color scale, from white (minimum) to red (maximum). **B**–**G** Dynamic changes to biofilm morphology in cells exposed to normal or inhibited geomagnetic field during 8 and 24 h of growth: **B**, **C** control *B. pumilus* under normal magnetic field; **D**, **E** control *B. pumilus* under inhibited (μ-metal) geomagnetic field; and **F**, **G** *B. pumilus* TezR–R2^{d} under inhibited (μ-metal) geomagnetic field. Images are representative of three independent experiments

and TezR–R2^{d} grown in the light presented altered margins, but their growth was contained compared with that of control *B. pumilus*.

As in the case of magnetoreception, we hypothesized that the reason for the observed phenotype was that *B. pumilus* TezR–R1^{d} and *B. pumilus* TezR–R2^{d} started responding to light only after 7 h, when either their RNA-based TezRs were restored or when the cell's normal response was restored after TezR destruction. Therefore, we analyzed the morphology of 7-h-old biofilms grown under light conditions (Fig. 10). By that time, biofilms of control *B. pumilus* already had an altered morphology compared with those grown in the dark. In contrast, the morphology of *B. pumilus* TezR–R1^{d} was identical irrespective of illumination conditions. Accordingly, changes to biofilm morphology of *B. pumilus* TezR–R1^{d} occurred within 7–24 h of growth in the light, when TezR–R1 should have already been restored.

Together, the results imply that TezRs are involved in the regulation of microbial light sensing. Specifically, we found a positive association between the ability of bacteria to sense and respond to light, and the presence of RNA-based TezRs.

Effect of TezRs on the anaerobic growth of aerobes

Intuitively, we hypothesized that TezRs might take part in the bacterial response to a changing gas composition. To test this hypothesis, we used the obligate aerobe *P. putida*, generally known for its inability to perform anaerobic fermentation. Introduction of numerous additional genes, a massive restructuring of its transcriptome, and nutrient supplementation have been proposed as the only means to accommodate anoxic survival of this species [66–69].

Control *P. putida* and *P. putida* lacking TezRs were placed on agar and cultivated under anoxic conditions. While control *P. putida*, and *P. putida* deficient in TezR–D1 or TezR–D2 alone, or in combination with loss of RNA-based TezRs, could not grow under anaerobic conditions, loss of only RNA-based TezRs allowed for anaerobic growth of *P. putida* (Fig. 11A,)B). *P. putida* TezR–R1^{d} and TezR–R2^{d} were characterized by microcolonies crowding (Fig. 11A, B).

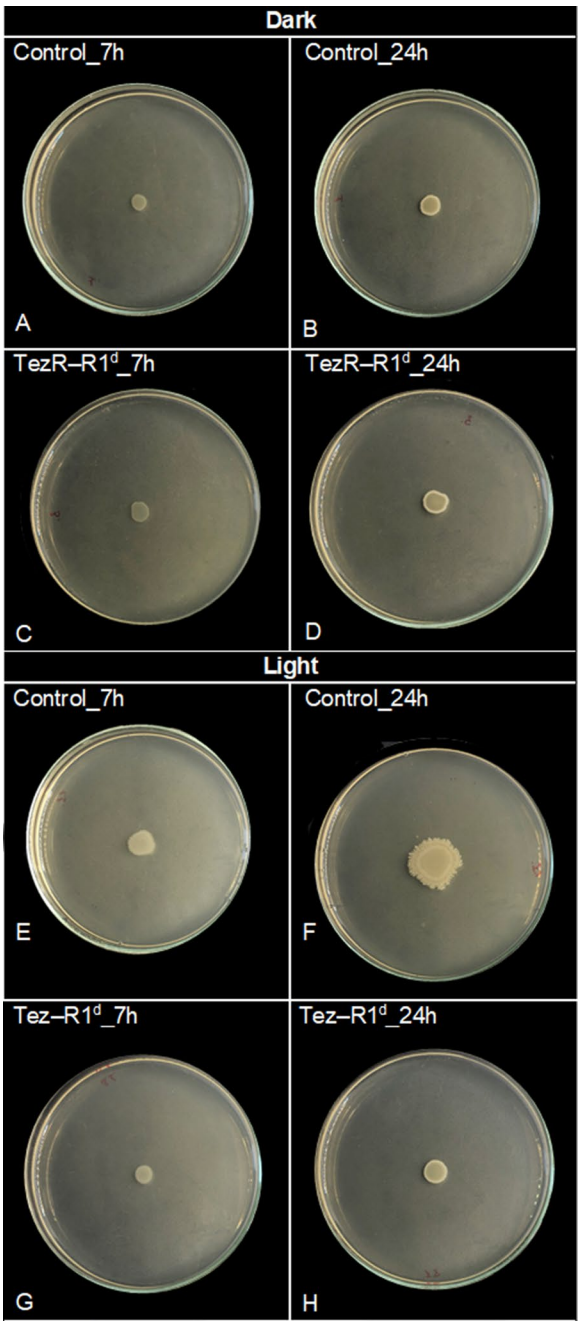

Fig. 10 Role of TezRs in light sensing. **A**–**D** Images of (**A**, **B**) control *B. pumilus* (Control) and (**C**, **D**) *B. pumilus* TezR–R1^{d} (TezR–R1^{d}) incubated in the dark for 7 h and 24 h. **E**–**H** Images of **E**, **F** control *B. pumilus* and **G**, **H** *B. pumilus* TezR–R1^{d} incubated in the light for 7 h and 24 h. Representative images of three independent experiments

We compared the biochemical profile of *P. putida* TezR–R2^{d} grown in anoxic conditions with control *P. putida* and aerobically grown *P. putida* TezR–R2^{d} using the VITEK® 2 system (Fig. 11C). We observed activation of the urease enzyme in both aerobically and anaerobically grown *P. putida* TezR–R2^{d}. This enzyme is considered essential for anaerobic fermentation in this species [66]. Moreover, when *P. putida* TezR–R2^{d} were cultivated under anoxic conditions, we noted the activation of some aminopeptidases and glycolytic enzymes known to participate in microbial anaerobic survival in the absence of external electron acceptors such as oxygen [70–73].

Collectively, the findings point to a previously unknown sensing and regulatory function of the TC- system and, in particular, the role of TezR–R1 and TezR–R2 in adaptation to variations in gas composition. Importantly, loss of these TezRs enables obligatory aerobic *P. putida* to grow under anoxic conditions.

Bacterial chemotaxis and biofilm dispersal are controlled by TezRs

Bacterial chemotaxis and biofilm dispersal are essential for colonizing various environments, allowing bacteria to escape stress, migrate to a nutritionally richer environment, and efficiently invade a host [74–76]. Although *Bacillus* spp. is believed to rely on transmembrane chemoreceptors to detect environmental chemical stimuli and a kinase (CheA) and response regulator (CheY) to mediate downstream signals, it remains to be determined how the receptor senses such stimuli [77–79]. Moreover, the gene network and signal transduction pathways controlling bacterial dispersal remain largely unexplored.

Here, we examined the role of TezRs in bacterial chemotaxis and dispersal in motile *B. pumilus* VT1200.

Control *B. pumilus* grew on the agar surface as round biofilms (Fig. 12A); however, addition of human plasma as a chemoattractant, triggered directional migration towards the plasma (Fig. 12B). Visual examination of biofilms revealed that *B. pumilus* TezR–D1^{d} lost their chemotaxis ability, while *B. pumilus* TezR–R1^{d} triggered biofilm dispersal within the chemoattractant zone (Fig. 12C–E). Biofilms formed by *B. pumilus* TezR–D2^{d} along with expanded biofilm growth, which appeared typical for this bacterium after the loss of TezR–D2^{d}, displayed marked chemotaxis towards plasma (Fig. 12F). Loss of TezR–R2 induced marked biofilm dispersal towards the chemoattractant (Fig. 12G) and was accompanied by the formation of multiple separate colonies in the agar zone where plasma was added. Combined elimination of both DNA- and RNA-based secondary TezRs maintained biofilm expansion and chemotaxis behavior (Fig. 12H) typical of *B. pumilus* TezR–D2^{d}; however, the primary community was characterized by zones of active sporulation (Additional file 7: Fig. S2).

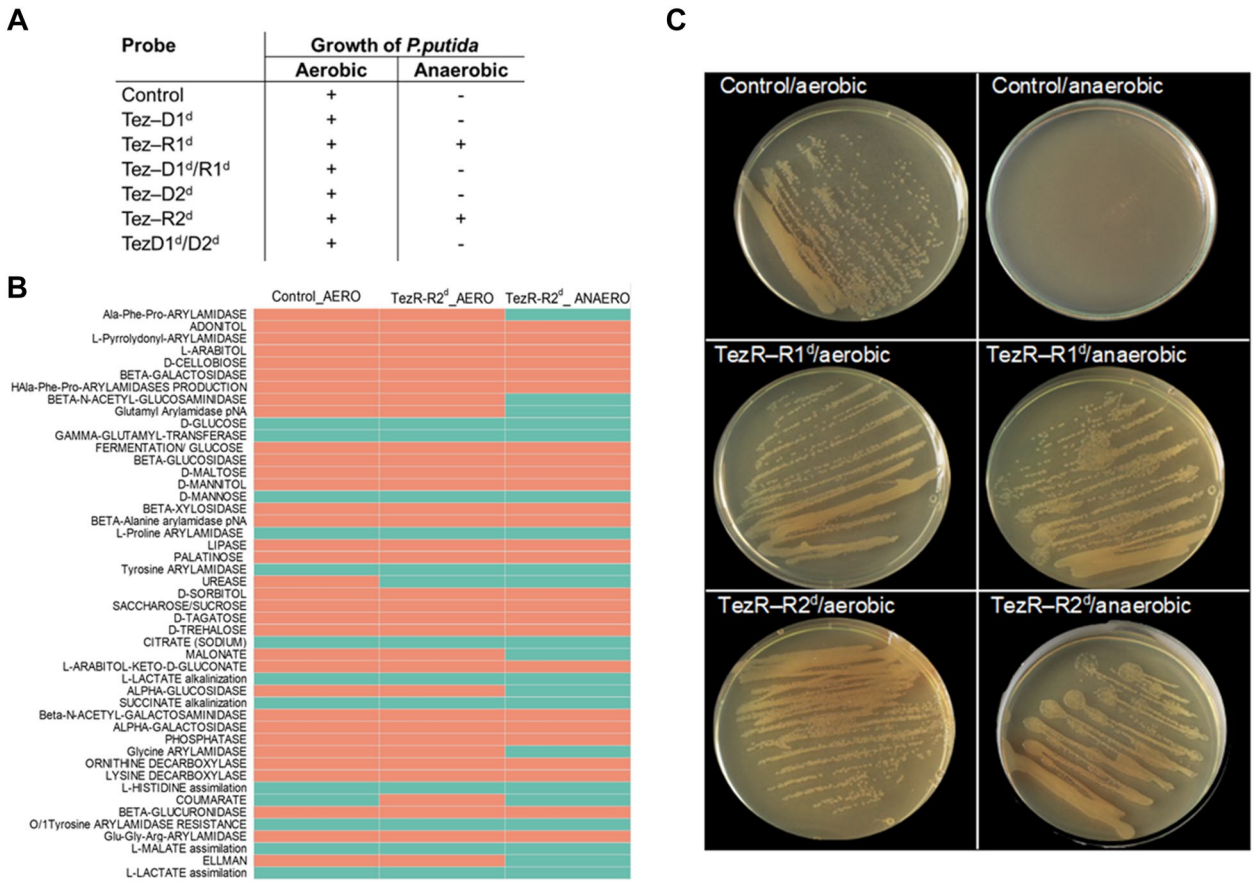

Fig. 11 Role of TezRs in growth of *P. putida* under anaerobic conditions. **A** Effect of TezRs loss on the growth of *P. putida* under aerobic and anaerobic conditions. Presence of bacterial growth is marked with a "+" sign, absence of bacterial growth is marked with a "—" sign. Values correspond to representative results of three independent experiments. **B** Growth of control *P. putida*, *P. putida* TezR–R1^{d}, and *P. putida* TezR–R2^{d} under aerobic or anaerobic conditions for 24 h. **C** Biochemical profile of control *P. putida* grown under aerobic conditions (Control–aero) and *P. putida* TezR–R2^{d} cultivated under aerobic (TezR–R2^{d}–aero) and anaerobic (TezR–R2^{d}–anaero) conditions in a VITEK® 2 system. Green color denotes positive test reaction results, red color denotes negative results. Values correspond to representative results of three independent experiments

Interestingly, combined removal of primary and secondary DNA-based TezRs did not affect chemotaxis (Fig. 12I); however, *B. pumilus* TezR–D1^{d}/D2^{d} displayed geometrical swarming motility patterns with branched biofilm morphology, not observed in any other TezRs mutant of *B. pumilus*. Surprisingly, loss of all primary and secondary TezRs of *B. pumilus* prevented growth towards the chemoattractant, leading instead to negative chemotaxis away from plasma, and appearance of zones of active sporulation (Fig. 12K). These results point to the unique individual sensory and regulatory properties of TezRs in mediating chemotaxis, biofilm morphology, and dispersal. Biofilm dispersal triggered by the removal of TezR–R1 and TezR–R2 in the presence of chemoattractant occurred only in intact DNA-based TezRs. Hence, bacterial interaction with the chemoattractant is regulated by the TR-system through apparent cooperation between RNA- and DNA-based TezRs, as evidenced by the complex responses triggered by the loss of multiple TezRs, and which cannot be accounted for by summing up the effects of individual TezR inactivation.

TezRs regulate bacterial virulence

Membrane-damaging toxins that cause hemolysis or lecithin hydrolysis are critical for *S. aureus* virulence; however, regulation of their functioning remains poorly understood [80]. In accordance with the observed pluripotent regulatory role of TezRs, we investigated the effect of TezRs inactivation on the hemolytic and lecithinase activities of *S. aureus* SA58-1. Loss of TezR–D1 or TezR–D2 alone, or in combination with other TezRs, statistically inhibited hemolysis ($p < 0.05$) and triggered the switch from α-hemolysis to β-hemolysis (Fig. 13A), pointing to the activation of genes encoding different hemolysins.

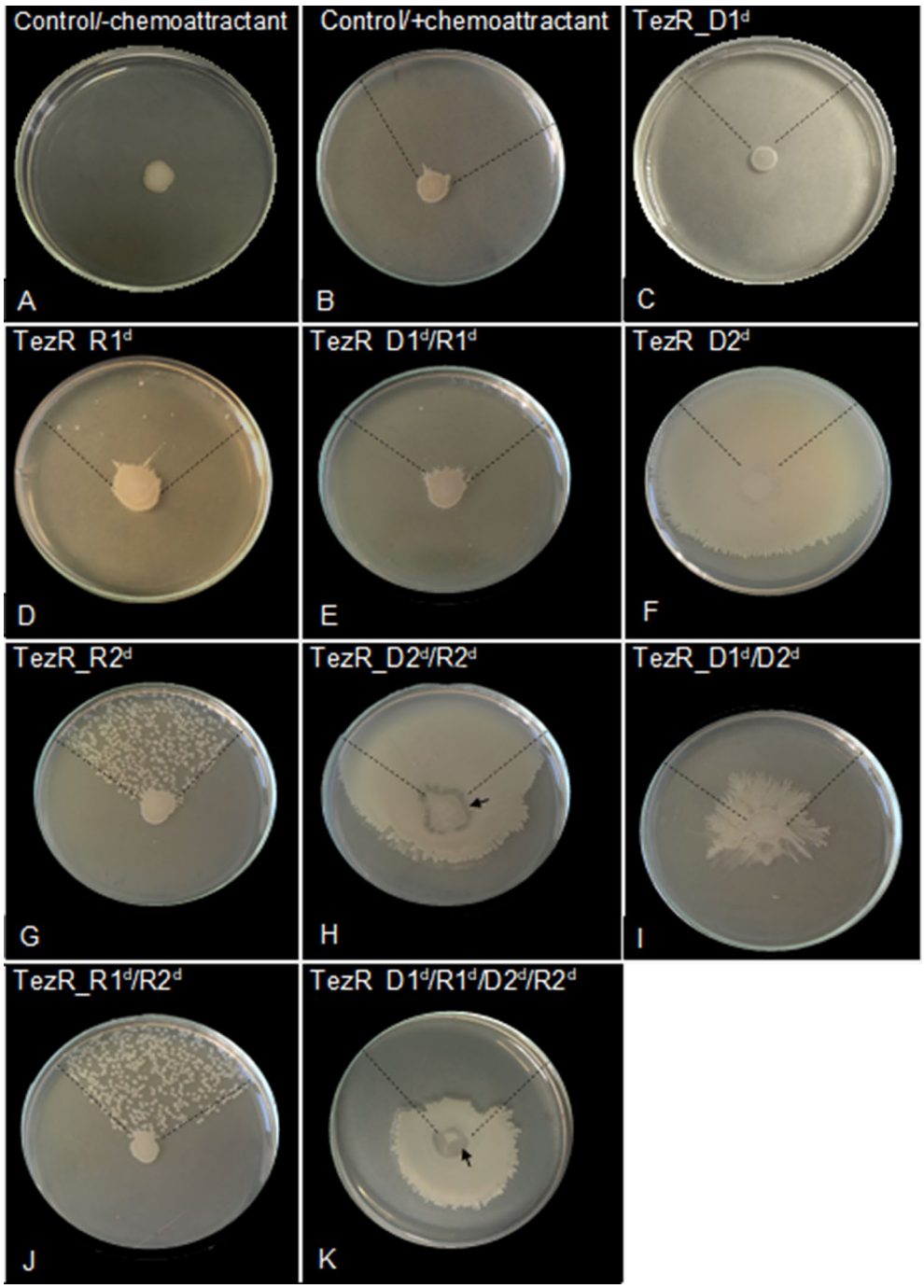

Fig. 12 Effect of TezRs on *B. pumilus* chemotaxis to plasma and biofilm dispersal. **A** Control *B. pumilus* with no chemoattractant added. **B** Chemotaxis of control *B. pumilus* towards plasma as chemoattractant. **C** Chemotaxis of *B. pumilus* TezR–D1^{d}. **D** Biofilm dispersal and chemotaxis of *B. pumilus* TezR–R1^{d}. **E** Chemotaxis of *B. pumilus* TezR–D1^{d}/R1^{d}. **F**, **H** Chemotaxis and visibly expanded biofilm growth of *B. pumilus* TezR–D2^{d} and *B. pumilus* TezR–D2^{d}/R2^{d}. **G**, **J** Chemotaxis and intense biofilm dispersal of *B. pumilus* TezR–R2^{d} and *B. pumilus* TezR–R1^{d}/R2^{d}. **I** Chemotaxis of *B. pumilus* TezR–D1^{d}/D2^{d}. **K** Negative chemotaxis of *B. pumilus* TezR–D1^{d}/R1^{d}/D2^{d}/R2^{d}. Black dotted lines denote the area in which plasma was placed. The black arrow points to zones of active sporulation. A chemotactic response is visualized as a movement of the biofilm away from the center towards the chemoattractant. Representative images of three independent experiments

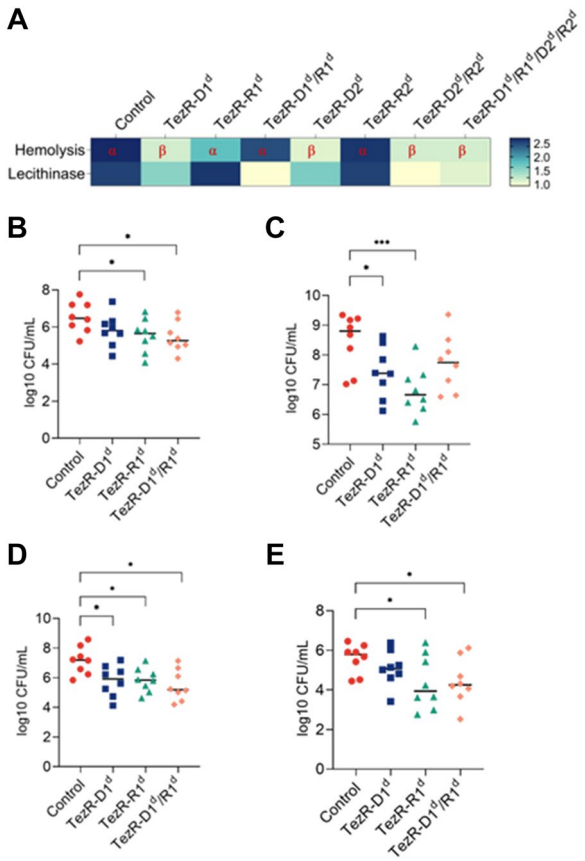

Fig. 13 Role of TezRs in virulence. **A** Role of TezRs in the of *S. aureus* hemolysis and lecithinase activities. Hemolytic activity of control *S. aureus* or *S. aureus* lacking TezRs is represented by a clear zone around the colonies on sheep blood agar plates. The presence of α- or β-hemolysis is marked with red letters. Lecithinase activity was analyzed by measuring a white diffuse zone surrounding the colonies. The extent of hemolysis and lecithinase zones (in mm) ranges from white (minimal) to dark blue (maximum). **B**–**E** Bacterial burden in animals intraperitoneally challenged either with control *S. aureus*, *S. aureus* TezR–D1^{d}, *S. aureus* TezR–R1^{d} or *S. aureus* TezR–D1^{d}/R1^{d}. Mice (n = 8) were euthanized 12 h after inoculation and ex vivo CFU were determined in **B** abdominal fluid, **C** liver, **D** spleen, and **E** kidneys. Values represent the mean ± SD. Each symbol corresponds to an individual mouse; horizontal bars denote the geometric mean. *p < 0.05, **p < 0.001

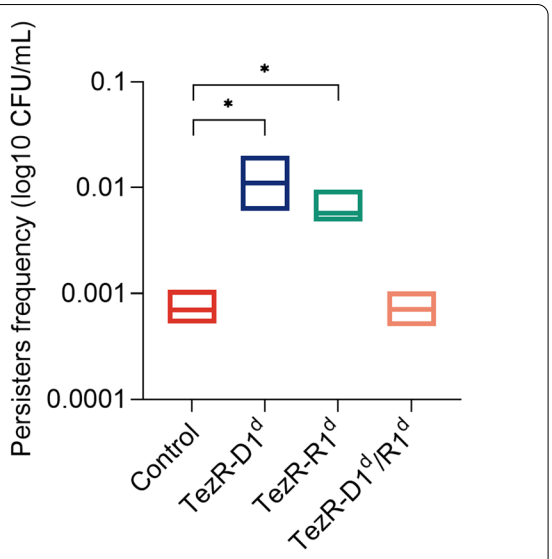

Fig. 14 Impact of TezRs on persister formation. Control *E. coli*, *E. coli* TezR–D1^{d}, *E. coli* TezR–R1^{d}, and *E. coli* TezR–D1^{d}/R1^{d} were exposed to ampicillin for 6 h at 37 °C in LB broth and plated on LB agar without antibiotics to monitor CFU counts and colony growth. Values are representative of three independent experiments. Bars represent the mean ± SD. *p < 0.05

A similar pattern was observed regarding the role of TezRs in regulating lecithinase activity (Fig. 13A), which was also inhibited following loss of DNA-based TezRs alone or in combination with RNA-based TezRs (p < 0.05). In contrast, inactivation of TezR–R1 or TezR–R2 alone caused no statistically significant alterations of hemolytic and lecithinase activities.

To further clarify the role of TezRs in virulence, we used a mouse model of *S. aureus* peritoneal infection. Mice were intraperitoneally challenged with 10.1 log10 CFU/mouse containing control *S. aureus*, *S. aureus* TezR–D1^{d}, *S. aureus* TezR–R1^{d} or *S. aureus* TezR–D1^{d}/R1^{d} (Fig. 13B–E). All animals exhibited typical signs of acute infection within 12 h, including hypothermia, hunched posture and slightly reduced movement, piloerection, breathing difficulty, narrowed palpebral fissures, trembling, and reduced locomotor activity. Bacterial load was measured in the abdomen, spleen, liver, and kidneys 12 h post infection by aspiration from the abdomen or homogenization of organs, plating on selective *S. aureus* medium, and subsequent identification by microscopy.

Loss of any of the primary TezRs altered the host-parasite relationship, decreasing dissemination of *S. aureus*. The most pronounced decrease was observed in the liver, kidney, and spleen in the group challenged with *S. aureus* TezR–R1^{d}. Reduction of *S. aureus* dissemination was less clear following infection with *S. aureus* TezR–D1^{d} or *S. aureus* TezR–D1^{d}/R1^{d}, although it nevertheless resulted in a significant drop in viable counts in some organs. Taken together, these results imply that bacteria are disseminated less effectively following the deactivation of TezRs, which can be associated with their higher susceptibility to the host immune response or altered adaptation to the environment.

Formation of bacterial persisters can be managed by TezRs

To gain insight into how TezRs regulated the formation of persisters, we used *E. coli* ATCC 25,922. Control *E.*

Table 2 Role of TezRs in spontaneous RifR mutagenesis

Probe	RifR mutants per 9 log10 *E. coli* cells (mean ± SD)[a]	P value
Control *E.coli*	27 ± 5.79	
E.coli TezR–D1^d	0 ± 0	0.015
E.coli TezR–R1^d	34 ± 8.84	0.249
E.coli TezR–D1^d/R1^d	1050 ± 258.83	0.021

[a] Values represent the mean from at least three independent experiments

coli, *E. coli* TezR–D1^d, *E. coli* TezR–R1^d, and *E. coli* TezR–D1^d/R1^d were normalized with respect to CFU, diluted in fresh ampicillin-containing medium, and incubated for 6 h (Fig. 14). The number of viable cells in the culture was determined by plating them on agar and overnight incubation.

As expected, only 1/1304 of original control *E. coli* cells were ampicillin tolerant. Primary TezRs regulated the rate at which cells entered dormancy and defined the persistence rate. The number of persisters was 155 times higher in *E. coli* TezR–D1^d and 8.5 times higher in *E. coli* TezR–R1^d (Fig. 14). Notably, the combined loss of both primary DNA- and RNA-based TezRs did not affect persister formation and there was no difference in the number of persisters between "Drunk" *E. coli* TezR–D1^d/R1^d and the control.

Dependence of spontaneous mutagenesis from TezRs

Next, we examined how the destruction of different TezRs affected the rate of spontaneous mutagenesis. In these experiments, we measured spontaneous mutation frequency to rifampicin in *E. coli* ATCC 25922 by counting viable RifR mutants after cultivation on rifampicin-supplemented agar plates (Table 2). Spontaneous mutagenesis was inhibited in *E. coli* TezR–D1^d, meaning that inactivation of TezR–D1 blocked the occurrence of replication errors, while loss of TezR–R1 did not affect this process. Surprisingly, the combined loss of TezR–D1/R1 triggered spontaneous mutagenesis and led to significantly more RifR mutants in "Drunk" *E. coli* TezR–D1^d/R1^d.

Inactivation of TezRs favors bacterial recombination

To determine the role of TezRs in bacterial recombination, we incubated control *E. coli* LE392 with λ phage (bearing Ampr and Kanr genes) for a time sufficient to cause phage adsorption and DNA injection. This was followed by treatment with nucleases to generate *E. coli* LE392 TezR–D1d, *E. coli* LE392 TezR–R1^d, and *E. coli* LE392 TezR–D1^d/R1^d ([51]).

Control *E. coli* LE392 were incubated with λ phage, but were not treated with nucleases. Loss of any primary TezRs increased recombination frequency, as indicated

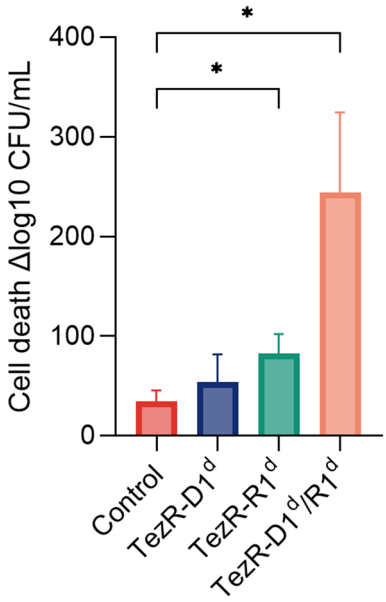

Fig. 15 Role of TezRs in bacteriophage integration frequency. Data represent the mean of three independent experiments, error bars depict the standard deviation. *p < 0.05

by the increased rate at which phages lysogenized sensitive bacteria and, consequently, the higher number of antibiotic-resistant mutants (Fig. 15). The increase was statistically significant ($p < 0.05$) only in bacteria lacking TezR–R1 or those with combined inactivation of TezR–D1/R1. Taken together, these findings show that primary TezRs regulate recombination frequency and their loss can affect prophage formation.

TezRs manage xenobiotic utilization

To investigate the role of TezRs in xenobiotics utilization, control *B. pumilus* and *E. coli* or their counterparts lacking primary TezRs were inoculated in M9 minimal medium supplemented with the xenobiotic dexamethasone as the sole source of carbon and energy [81, 82]. We compared the lag phase, which comprises the time required for sensing and starting the utilization of these nutrients, between bacteria with unaltered and destroyed primary TezRs [58, 59, 83].

Inactivation of TezR–D1 in *E. coli* and *B. pumilus* did not affect the lag phase when bacteria were grown on media supplemented with dexamethasone. In marked contrast, the time lag of *E. coli* and *B. pumilus* devoid of TezR–R1 (Fig. 16A, B) was delayed by 3 and 2 h compared with that of control bacteria ($p < 0.05$), indicating a delay in the uptake and consumption of dexamethasone.

We hypothesized that the prolonged time required by bacteria lacking TezR–R1 to start using dexamethasone resulted from disruption of their role in controlling

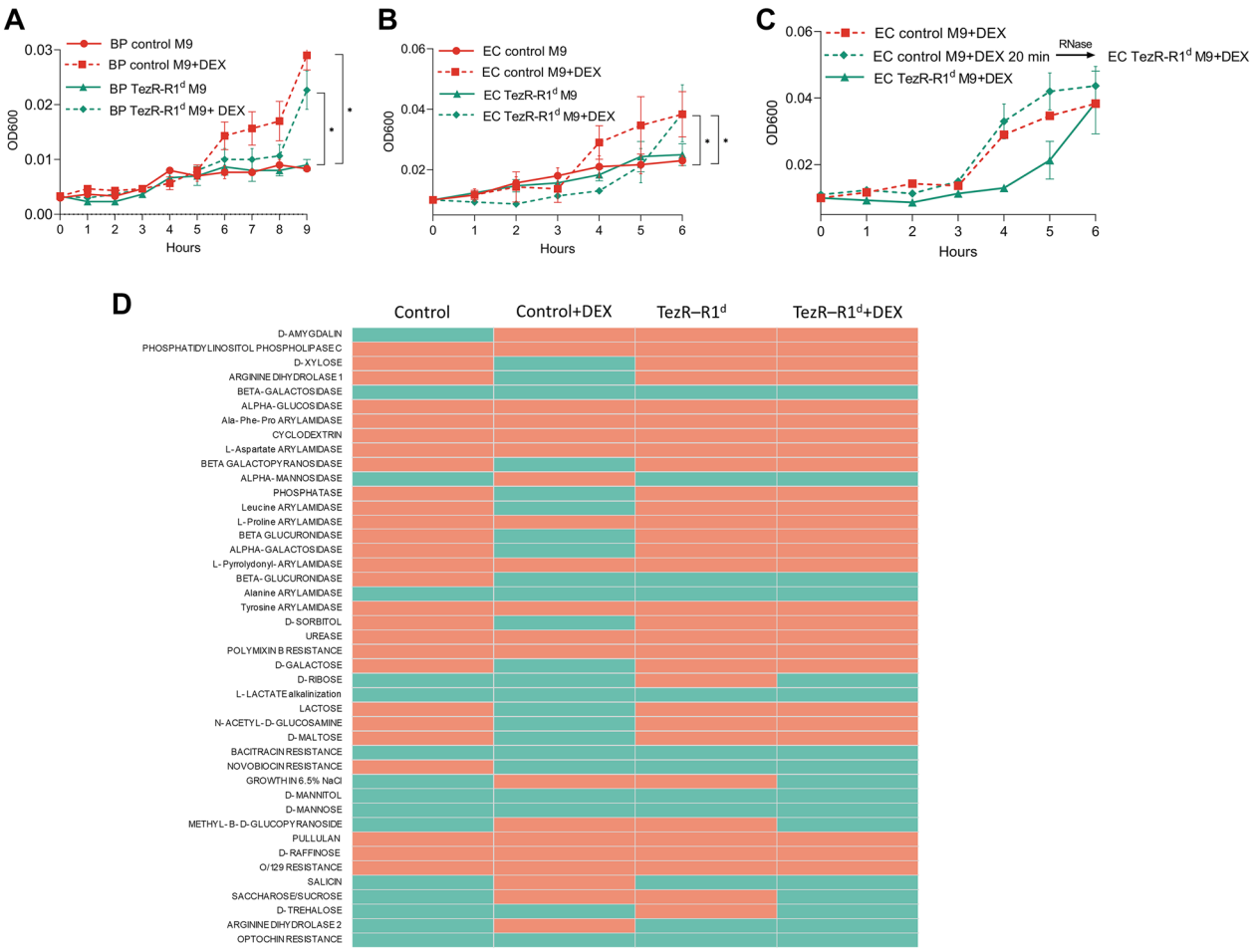

Fig. 16 Role of TezRs in chemosensing and bacterial memory. Growth of control *B. pumilus* or *E. coli* and their counterparts lacking primary TezRs on M9 medium with and without dexamethasone (DEX) or lactose (LAC) was monitored over time. **A** Control *B. pumilus* and *B. pumilus* TezR–R1^{d} grown in M9 medium with or without dexamethasone. **B** Control *E. coli* and *E. coli* TezR–R1^{d} grown in M9 medium with or without dexamethasone. **C** Pretreatment of control *E. coli* with dexamethasone for 20 min followed by TezR–R1 removal and subsequent growth on M9 medium supplemented with dexamethasone. **D** Biochemical profile of control *B. pumilus* and *B. pumilus* TezR–R1^{d} grown on minimal M9 medium without (M9) or with dexamethasone (M9 + DEX). Green denotes positive test reaction results, red denotes negative results. Values show representative results of three independent experiments. **E** Control *E. coli* and *E. coli* TezR–R1^{d} grown in M9 medium with or without lactose. **F** Pretreatment of control *E. coli* with lactose for 20 min followed by TezR–R1 removal and subsequent growth on M9 medium supplemented with dexamethasone. **G** Time required for dexamethasone-naïve and dexamethasone-sentient control *E. coli* to commence growth on M9 medium supplemented with dexamethasone. **H** Time required for dexamethasone-naïve and dexamethasone-sentient control *B. pumilus* to commence growth on M9 medium supplemented with dexamethasone. **I** Minimal time required for *E. coli* to start utilization of dexamethasone. The X-axis represents the time lag of control *E. coli* upon initial and second exposure to DEX. **J** Time to the start of DEX utilization (t_{lag}) by dexamethasone-naïve and dexamethasone-sentient *B. pumilus*. The experimental protocol is shown to the left. The t_{lag} after each passage in nutrient broth with or without dexamethasone is shown to the right as a heat map, whose color scale ranges from white (0 h) to red [5 h]. **K** Minimal time required for *B. pumilus* to start dexamethasone utilization after one-two or three times destruction of TezR–R1

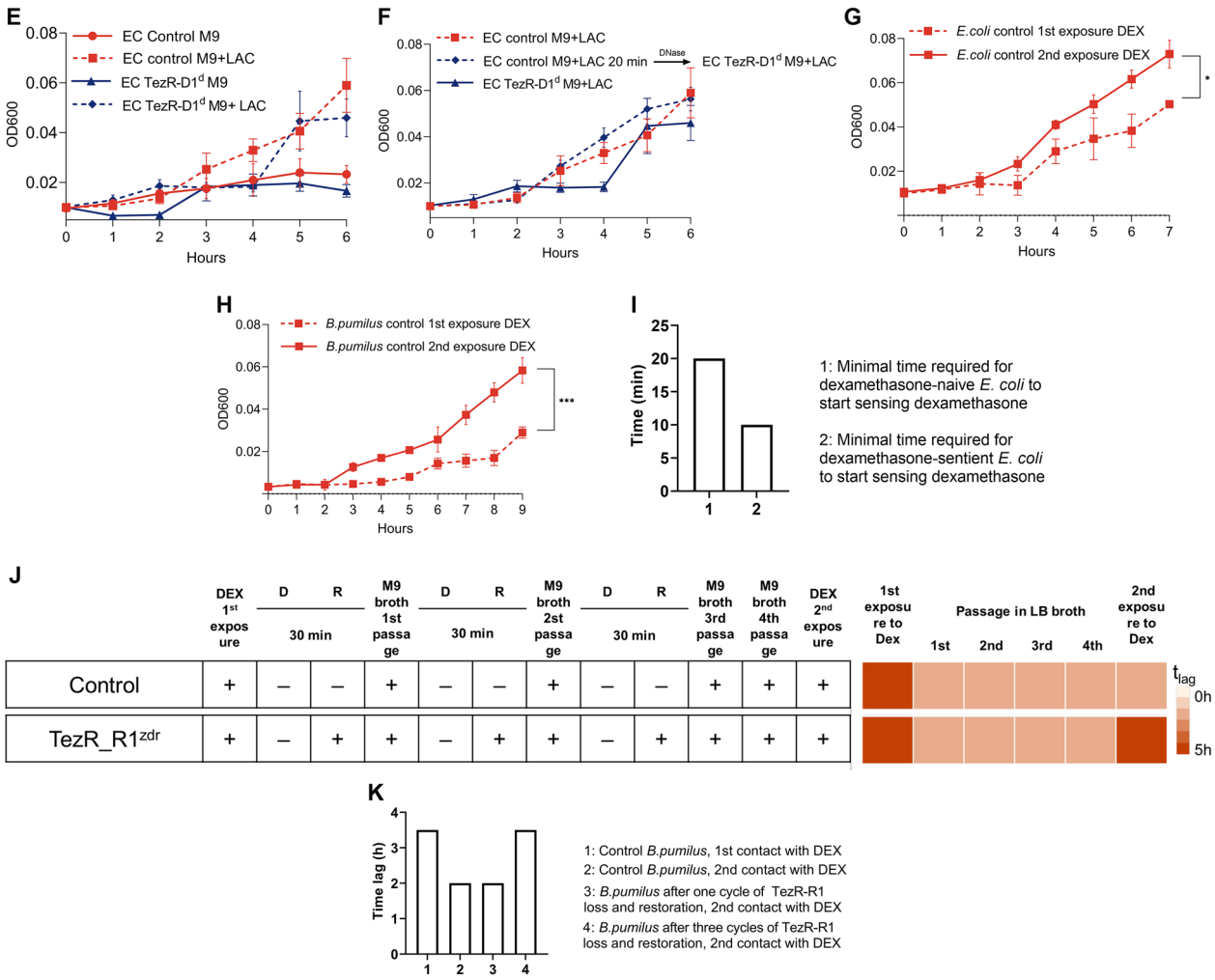

Fig. 16 continued

nutrient consumption, rather than an alteration of transcriptional activity following their removal that could affect nutrient factor utilization. To verify this hypothesis, we conducted an experiment designed to prove that if TezR–R1 is implicated in dexamethasone utilization, then *E. coli* pretreated with dexamethasone followed by TezR–R1 elimination and cultivation in M9 supplemented with dexamethasone would have the same time lag as wild-type *E. coli* in the same M9 medium. In other words, the presence of TezR–R1 is a prerequisite for bacteria to sense and utilize dexamethasone and once bacteria with unaltered TezR–R1 sense dexamethasone, they continue utilizing it even if TezR–R1 is subsequently removed.

In agreement with this hypothesis, control *E. coli* exposed to dexamethasone for at least 20 min with subsequent TezR–R1 loss and inoculation in dexamethasone-supplemented M9 exhibited similar growth and time lag as control *E. coli* (Fig. 16C).

We also analyzed how inactivation of TezR–R1 altered the biochemical profile of *B. pumilus* grown on minimal M9 medium supplemented with dexamethasone (Fig. 16D). Addition of dexamethasone to control *B. pumilus* clearly induced a variety of enzymes known to participate in steroid metabolism including β-glucuronidase [84]. This increase was less apparent in *B. pumilus* TezR–R1^{d}, whereby no β-glucuronidase was detected. The lack of changes in the biochemical

activity of bacteria devoid of TezRs following treatment with nutrients provides another line of evidence supporting the essential role of TezRs in managing xenobiotic utilization.

Utilization of lactose and functioning of the lac-operon are controlled by TezRs

To evaluate the potential universal role of primary TezRs in detecting exogenous nutrients, we examined their role in lactose metabolism by cultivating the lac-positive strain E. coli ATCC 25,922 in M9 medium supplemented with lactose as the sole source of carbon and energy. Surprisingly, unlike for dexamethasone, inactivation of TezR–R1 had no effect on lactose utilization. At the same time, loss of TezR–D1 increased the time lag by 2 h compared with control *E. coli*, indicating that utilization of lactose was regulated by these receptors (Fig. 16E). As with dexamethasone, when control E. coli were pre-exposed to lactose for 20 min, followed by TezR–D1 removal and subsequent cultivation on M9 medium supplemented with lactose, their behavior and time lag was similar to that of control E. coli (Fig. 16F). This finding further confirmed the supervised role of TezR–D1 in lactose metabolism over lac-operon.

TR-system is implicated in bacterial memory and forgetting

We reasoned that, if TezRs participated in the consumption of nutrients, they might also play a role in bacterial memory formation and verified this possibility using an 'adaptive' memory experiment [19, 85]. We found that control *E. coli* and *B. pumilus* "remembered" the first exposure to dexamethasone, as indicated by shortening of the lag phase from 3 h upon first exposure to 2 h upon second exposure for *E. coli* and from 5 to 2 h for *B. pumilus* (Fig. 16G, H).

We next assessed whether TezRs implicated in the memorization of a previous engagement to nutrients required less time to trigger utilization of such a nutrient upon repeated sensing. To achieve the stated goal, we exposed "dexamethasone-naïve" and "dexamethasone-sentient" *E. coli* with unaltered TezRs to dexamethasone for different time periods. After that, TezR–R1 were destroyed and cells were placed in fresh M9 medium containing dexamethasone. Only the bacteria whose pre-exposure to dexamethasone prior to TezR–R1 destruction was enough to trigger its utilization were able to grow. In agreement with our hypothesis, we found that TezR–R1 required 20 min to trigger the utilization of dexamethasone upon first exposure to it (Fig. 16)I), but only 10 min upon second exposure ($p < 0.05$). The difference in time required for TezR–R1 to mount a response at first (20 min) and repeated (10 min) contact with

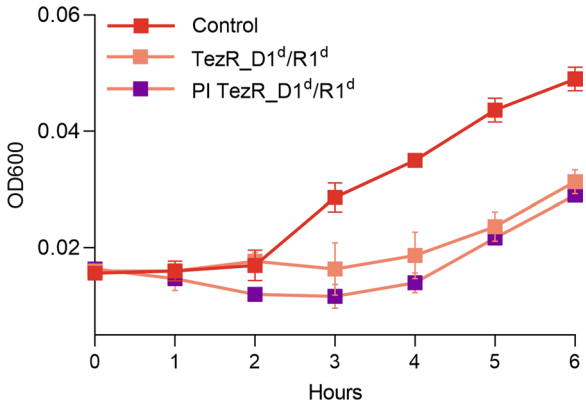

Fig. 17 Inactivation of TezRs with PI

dexamethasone points to the involvement of TezRs and the TRB-receptor system in long-term cell memory formation, enabling a faster response to repeated stimuli [86].

We next studied the role of TezRs in "forgetting". We supposed that because TezRs participated in bacterial memory, their continued loss might result in no memory of past experiences, which would reflect in a longer time lag.

We found that control *B. pumilus* remembered the first exposure to dexamethasone, indicated by reduction of the lag phase from 5 h upon first exposure to 2 h upon second exposure. Dexamethasone-sentient *B. pumilus* with restored TezRs (following one- or two-time cycles of TezRs removal and subsequent restoration) maintained a time lag below 2 h (Fig. 16J), meaning that these one- or two-time cycles of TezRs loss did not affect bacterial memory. However, three repeated rounds of TezRs removal and restoration led to "forgetting" of any previous exposure to dexamethasone and the behavior of the corresponding *B. pumilus* became similar (5-h lag phase) to that of control *B. pumilus* upon first exposure to dexamethasone. We named these cells, whose memory had been erased by multiple cycles of TezRs loss "Zero cells".

Moreover, we found that after one or two-time removal of TezRs and subsequent restoration, cells continued to react faster to the substrate than at the very first contact (Fig. 16K). However, *B. pumilus* with TezRs restored after three-time cycles destruction required the same contact time as naïve cells to sense and trigger substrate utilization. We reasoned that cells with TezRs restored after one- or two-time cycles of destruction retained a type of "memory" (a reduced time required to launch substrate utilization). This phenomenon appeared to depend on the role of TezRs in a bacterial intergenerational memory scheme capable of maintaining and losing past histories of interactions.

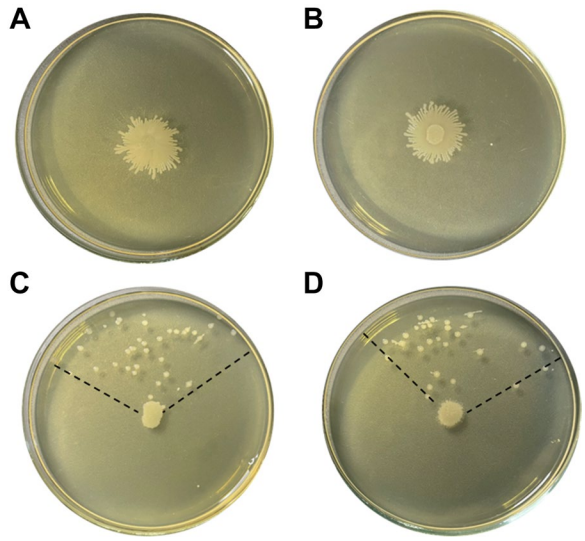

Fig. 18 Inactivation of TezRs with anti-DNA and anti-RNA antibodies. Morphology of 24 h old biofilms formed with anti-DNA or anti-RNA antibodies or nucleases added to the agar. **A** *B. pumilus* cultured on the agar supplemented with anti-DNA antibodies. **B** *B. pumilus* supplemented with DNase (TezR–D2^{d}). **C**–**D** Effect of inactivation or destruction of TezR-R2 on directional migration of *B. pumilus* to plasma used as a chemoattractant (**C**) *B. pumilus* cultured on the agar supplemented with anti-RNA antibodies. **D** *B. pumilus* supplemented with RNase (TezR–R2^{d}). Black dotted lines denote the area in which plasma was placed

The effect of the binding of propidium iodine (PI) on the functionality of TezRs

To further confirm the role of TezRs in cell signaling we inactivated them using PI, which is known to bind both DNA and RNA without penetrating the live cells [87]. Similar to the observation where both TezR–D1^{d}/R1^{d} were removed, PI-treated *B. pumilus* exhibited the identical pattern of increase in lag phase and delay in the uptake of dexamethasone when incubated in minimal media (Fig. 17). Thus, these results imply that both TezR destruction and the deactivation of their functions by PI binding modulate the sensory and regulatory activities of the cell.

Time required for dexamethasone-sentient *B. pumilus* control (control), or *B. pumilus* following TezR–D1/R1 destruction (TezR–D1^{d}/R1^{d}) or with TezR inactivated with PI (PI TezR–D1^{d}/R1^{d}) to commence growth on M9 medium supplemented with dexamethasone. Data are representative of three independent experiments.

The effect of anti-DNA and anti-RNA antibodies on the functionality of TezRs

We next confirmed that the inhibition of secondary TezRs with anti-DNA and anti-RNA antibodies leads to identical consequences as their destruction with nucleases. When anti-DNA antibodies were added to the agar (Fig. 18A) and bound to TezR-D2, the biofilms of *B. pumilus* were characterized by the formation of dendritic-like colony patterns as seen in biofilms formed by bacteria after the loss of TezR–D2 (Fig. 18B). The inactivation of TezR-R2 with anti-RNA antibodies triggered the directional migration of *B. pumilus* (Fig. 18C) the same way as did the destruction of TezR-R2 with RNase added to the agar (Fig. 18D).

Role of reverse transcriptase and integrase in functioning of the TR-system

We hypothesized that formation and functioning of TezRs could be associated with reverse transcription and that affecting the corresponding enzymes might prevent the restoration of TezRs after their removal. Recent data suggest that non-nucleoside reverse transcriptase inhibitors (RTIs), originally designed to block HIV reverse transcriptase, interact non-specifically with different transcriptases [88, 89]. Here, we used non-nucleoside RTIs against control *S. aureus* and *S. aureus* lacking primary TezRs.

The RTIs etravirine and nevirapine did not exhibit any antibacterial activity against *S. aureus* and presented a MIC > 500 μg/mL (Additional file 5: Table S5). Thus, in this experiment we used very low doses of RTIs, more than 100 fold lower than their MICs.

Addition of RTIs to the medium did not alter growth dynamics of control *S. aureus* (measured as OD600), but affected growth of *S. aureus* lacking primary TezRs (Fig. 19A). Specifically, RTIs inhibited growth of *S. aureus* TezR–D1^{d} ($p < 0.05$ for all), but not *S. aureus* TezR–R1^{d}. Even more surprisingly, treatment of *S. aureus* TezR–D1^{d}/R1^{d} with RTIs accelerated bacterial growth. We suggest that the inhibitory effect of RTIs on growth of bacteria lacking TezRs can be explained by the requirement for these receptors when cells are grown in liquid media.

Next, we investigated the onset of a signal transduction cascade following the interaction between TezRs and ligands. We hypothesized that the response to stimuli might also depend on recombinases. To verify this possibility, we used raltegravir, an inhibitor of viral integrase known to cross-react with bacterial recombinases due to structural and functional similarity with HIV integrase [90, 91]. Using a nontoxic concentration of raltegravir (Additional file 5: Table S5), we successfully blocked the activation of bacterial enzymes of control *B. pumilus* in response to dexamethasone (Fig. 19B). As a result, the biochemical profile of control *B. pumilus* grown on M9 medium supplemented with dexamethasone and raltegravir was almost identical to that of *B. pumilus* grown on M9 without dexamethasone. This allowed us to

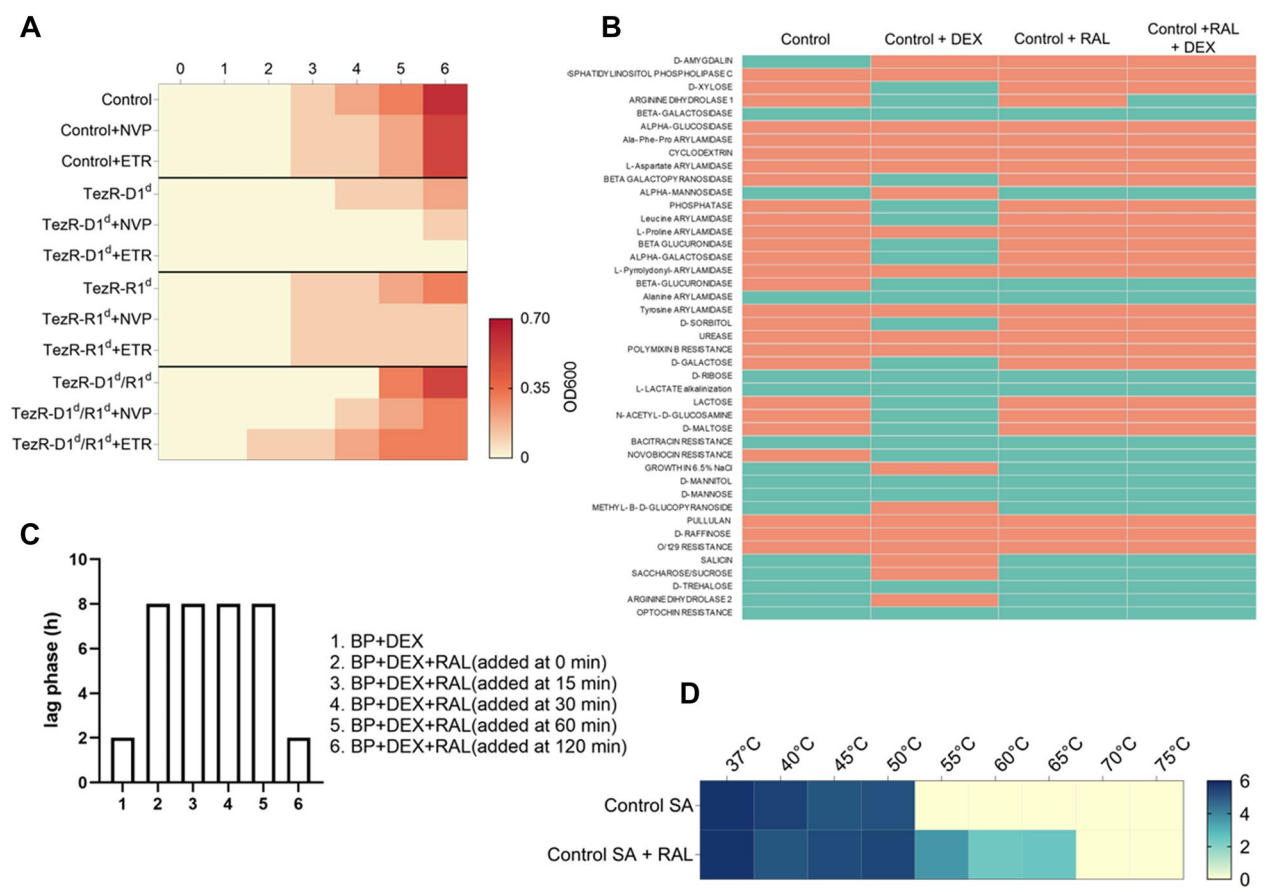

Fig. 19 Role of reverse transcriptase and integrase in the TC-system. **A** Effect of RTIs on bacterial growth and memory. Heat map representation of growth by control *S. aureus*, *S. aureus* TezR–D1^{d}, *S. aureus* TezR–R1^{d}, and *S. aureus* TezR–D1^{d}/R1^{d} upon treatment with RTIs. Nevirapine (NVP) and etravirine (ETR) were added to the broth and OD600 was monitored hourly for 6 h at 37 °C. OD600 is labeled by a color scale, from white (minimal) to red (maximum). Values show representative results of three independent experiments. **B** Biochemical profile of control *B. pumilus* grown on M9 minimal medium without (M9) or with dexamethasone (M9 + DEX), and with or without adding raltegravir (RAL). Green denotes positive test reaction results, red denotes negative results. Values show representative results of three independent experiments. **C** Raltegravir (RAL) added at different time points from 0 to 120 min to dexamethasone-sentient *B. pumilus* grown on M9 medium with dexamethasone (DEX). **D** Heat map showing the effect of raltegravir on signal transduction from TezRs in relation to temperature tolerance in control and raltegravir-treated (control + RAL) *S. aureus* (SA). CFU are labeled by a color scale, from white (minimum) to blue (maximum). Values show representative results of three independent experiments

assume that raltegravir could block signal transduction from TezRs following playing an identical role as TezRs loss.

To confirm that the raltegravir-inducted response of *B. pumilus* to dexamethasone was not the result of any toxic effect, we measured OD600 of control *B. pumilus* when raltegravir was added to the medium at different time points from 0 to 120 min (Fig. 19C). The addition of raltegravir to dexamethasone-sentient control *B. pumilus* grown on M9 with dexamethasone led to the inhibition of bacterial growth only when it was added before the first 60 min; the inhibitory function was lost when added after 120 min (Fig. 19C). We believe that raltegravir inhibited signal transduction from TezRs occurring during the first 120 h, but had no control over it once the signal had already been relayed.

Given that we previously showed how the loss of TezRs enhanced survival at higher temperatures, we hypothesized that raltegravir might block signal transduction from TezRs and lead to higher heat tolerance even in bacteria with intact TezRs. *S. aureus* treated or not with raltegravir were gradually heated up to 65 °C and the presence of viable bacteria was analyzed. *S. aureus* treated with raltegravir could survive at temperatures over 15 °C higher than those of cells not treated with raltegravir (Fig. 19D). These data add another line of evidence supporting that recombination processes

might be involved in the realization of different signals from TezRs within the TR-system.

Discussion

Here, we describe for the first time the most external receptive system in bacteria, named the "TR-system," which oversees various aspects of cell behavior, as well as cell memory. Such a universal receptive system, implicated in response to a wide range of chemical, physical, and biological factors, has not been described previously in prokaryotes; however, an identical system was recently discovered by our group in a variety of eukaryotic cells [45].

This system is composed of previously uncharacterized nucleic-acids based receptors, as well as reverse transcriptases and integrases. Our study shows a unique composition of these receptors, which we named TezRs. In contrast to known receptors formed by proteins, TezRs are formed by DNA and RNA molecules [92]. The selective inactivation of different TezRs led to individual alterations in cell functioning and remarkably impacted the transcription of various genes, which highlights the specific role of each of the discovered TezRs.

One can assume that nucleic acid–based TezRs are ancient regulatory elements, given that the evolutionary development of cells started from the cooperation of nucleic acids, RNA in particular [93].

We first showed that the TR-system functioned robustly across different bacterial types and played a previously unexplored and critical role in the management of microbial growth in liquid and solid media, as well as in collective behavior. These processes are known to be tightly regulated by numerous genes and post-transcriptional events [94]. Loss of different TezRs resulted in changes to growth kinetics, biofilm formation, and cell size. The most significant alterations were noted for biofilms formed by motile bacteria lacking TezR–D2. These biofilms were characterized by formation of dendritic-like colony patterns, typical of cells with an increased swarming motility. Given that swarming motility is a result of a previously unknown, but hypothetically existing system which is believed to sense bacterial interaction with a surface and transfer these signals to the cells, we can state that TezRs are likely to be these sensors that regulate this processes [95, 96].

Biofilm dispersal allows bacterial cells to leave a biofilm and migrate to a more favorable environment for resettlement. Previous evidence suggests that biofilm dispersal depends on surface sensing and is modulated by the alteration of environmental conditions or specific gene activity [56, 95, 97, 98]. However, our data validated that this process is also modulated by TezRs.

Another important event related to biofilm-related bacterial survival relies on the formation of persisters [52, 99, 100]. We also found that primary TezRs regulated the rate at which cells entered dormancy and determined the persistence rate, thereby defining a bet-hedging strategy of cells.

To evaluate the role of the TR-system in bacterial adaptation to a variety of chemical and physical factors, we began by looking at the regulation of bacterial survival at high temperatures. In a set of experiments, we showed that all primary TezRs (TezR–R1 in particular) were key regulators of survival under thermal stress, and their inactivation enabled mesophile bacteria (with an optimal growth temperature of 37 °C) to tolerate up to 20 °C higher temperatures than those managed by control bacteria. We reasoned that, because loss of TezRs before the heating step but not after increased survival, TezRs might be involved in thermosensing and supervise the corresponding response. Importantly, some previous studies highlighted that intracellular mRNA could act as a thermosensor and react to altered temperature by modulating translation [101]. We found that the TR-system orchestrated the cell response to UV exposure. When bacteria are exposed to UV light, they respond to DNA damage by a highly regulated series of events known as the SOS response, which ultimately dictates whether the cell should survive or induce cell death [102, 103]. The loss of RNA-based TezRs increased survival after UV exposure, which can be explained by the modulation of SOS response and the enhanced work of DNA repair system, or by modulation of damage tolerance and cell-cycle checkpoints [104–106].

An interesting finding regarding the regulation of cell responses to variations in gas composition was observed when the obligate aerobe *P. putida* could grow under anoxic conditions following the loss of TezR–R1 or TezR–R2. Notably, recent theoretical studies have suggested that the growth of *P. putida* under anoxic conditions would require numerous additional genes and a massive restructuring of its transcriptome to find alternative means of ATP synthesis [66, 68]. Therefore, we reasoned that the inactivation of RNA-based TezRs stimulates genomic variability, enabling the selection of clones capable of growing under anoxic conditions.

Furthermore, we observed that TezRs controlled sporulation, which represents another important bacterial indicator of the interaction to unfavorable environment and stress conditions [107, 108]. The most striking effects were observed in cells following the loss of TezR–R2, which increased sporulation, while the removal of TezR–D2 resulted in a total inhibition of sporulation in both standard and stress environments. The findings demonstrated that the TR-system supervises known regulatory

pathways and known receptors responsible for sporulation, exerting divergent effects on this process. Moreover, the loss of certain TezRs could either increase or totally inhibit this process.

Examining the bacterial response to other physical factors, we found that TezRs were involved in the response to changes in the geomagnetic field (known as magnetoreception) and light. Non-magnetotactic and non-photosynthetic *B. pumilus* with intact TezRs sensed inhibition of the geomagnetic field and the presence of light in the environment, as manifested by changes in biofilm morphology and expanded growth. We found that RNA-based TezRs are implicated in the interaction of cells with the geomagnetic field and light and that, in the case of their inactivation, bacteria could not start responding to alterations in these factors for a few hours, most likely until these TezRs were restored. It is surprising, since until now, the identity of a magnetic sensor in non-magnetotactic bacteria remained enigmatic; however, some studies show that different bacteria even lacking magnetosomes are capable of sensing the geomagnetic field [30, 31].

Interestingly, the ability of TezRs to interact with the magnetic field could be explained by the nucleic-acid structure of these receptors, owing to the alleged paramagnetic properties of nucleic acids and their ability to emit or transmit electromagnetic waves [109–113]. Also, the observed phenomenon of the overgrowth of non-magnetotactic bacteria in the case of the alteration of magnetic field is intriguing, particularly when considering the effect of strong magnetic exposures, such as MRI on human microbiota.

It has not escaped our attention that altered responses to these physical factors by bacteria with inactivated RNA-based TezRs were observed only as long as DNA-based TezRs were present. It is possible that different TezRs interact with each other to form functional network in which they affect each other's functioning. This observation corroborates the fact that selective or combined inactivation of various TezRs triggered different transcriptomic clustering. Notably, the most significant impact on the transcriptome profiles, with the upregulation of the highest number of genes was triggered by the individual loss of RNA-based TezRs.

Studying the role of the TR-system in response to different chemical and physical factors, we were surprised by how cells with inactivated RNA- and DNA-based TezRs continued responding to some of these factors. Although TezR–D1^{d}/R1^{d} bacteria displayed an increased survival at higher temperatures, their survival did not differ from that of control cells under altered UV, light, and gas content conditions. Indeed, combined cleavage of different TezRs triggered individual responses that were often more than just the sum of alterations triggered by the removal of each individual TezR. Thus, we named cells lacking primary DNA- and RNA-based TezRs that exhibited an unexpected response to stimuli "drunk cells." The paradoxical behavior of "Drunk cells" could be explained by the existence of internal (i.e., cytoplasmic) TezRs (TezR–i), which could be activated following the loss of primary TezRs. The existence of cytoplasmic receptors in bacteria was only recently shown, but these receptors are protein-based and respond only to chemosensing [114].

The present results also expanded our understanding of the TR-system in the control of mutational events and recombination frequency. We found that TezRs regulated spontaneous mutations and that it was possible to either inhibit this process through loss of TezR–D1 or increase it via combined removal of TezR–D1/R1. We did not look deeper into this phenomenon; however, we believe that alterations of these TezRs could possibly control the mismatch repair system, which is known to be responsible for spontaneous mutagenesis [115]. The control of bacterial variability by the TR-system is also supported by increased recombination frequency following TezRs deactivation during infections of bacteria by phages [116].

Our findings support a role for TR-system in microbial virulence and pathogenicity. TR-system regulate production of virulence factors, such as hemolysin and lecithinase, as well as in vivo bacterial dissemination. These properties are known to play an important role in the spreading of infections, but their underlying molecular mechanisms are only now beginning to be elucidated. In fact, given that inactivation of TezRs inhibited bacterial dissemination, nucleases produced by macroorganisms could actually constitute a protective mechanism [117, 118].

Finally, we studied the role of TR-system in bacterial chemotaxis, which is one of the primary means of bacterial adaptation [42]. We found that TR-system controlled chemotaxis and that removal of certain TezRs could either promote or inhibit this process, or even cause a switch from positive to negative chemotaxis. Because the loss of TezRs have not inhibited bacterial motility but modulated chemotaxis, we conclude that TR-system control and oversee the function of transmembrane methyl-accepting chemotaxis proteins, which are believed to be the primarily sensors and regulators of chemotaxis [119]. We found that the existence of TezRs was a prerequisite for different bacteria to utilize well-recognized factors such as lactose, as well as synthetic xenobiotics. The fact that utilization of different nutrient factors, including lactose depends on TezRs can be explained by the overseeing function

of the TR-system over different pathways including the lac-operon.

Summarizing, based on our results we hypothesize that the TR-system upon encountering a chemical or physical factors known to the cell regulates the work of existing pathways for their utilization or adaptation and, in the case of the absence of such a pathways, stimulates genome changes, which may contribute to the emergence of a novel pathways to respond to these factors.

The ability of cells to sense environmental factors and nutrients is also related to cell memory. Participation of TR-system in cell memory formation to known nutrients and xenobiotics was supported by the difference in time required to trigger substrate utilization by naïve and sentient bacteria. Given that cell memory formation is accompanied by genome rearrangement, and as we confirmed for the first time that they could be modulated by TezRs, it appears that TezRs might modulate genome rearrangement [120]. Intriguingly, our results showed that sentient bacteria exhibited faster substrate recognition than naïve cells and that this difference could be passed on through multiple generations which is controlled by TR-system. It is tempting to speculate that TR-system participate in memory formation to previous interactions of cells which leads to the synthesis of TezRs with memory to previous events and genes required for response. These characteristics shares similarity with the adaptive strategy of immune cells, whose secondary and more pronounced response is based on their affinity for antigens and the higher number of cells possessing relevant receptors [121–123].

In our study, three repeated rounds of TezRs loss led to "forgetting" of the initial contact with the substrate. We named such cells "Zero cells". "Zero cells" did not "remember" previous interactions with the substrate and required the same time to start its utilization as substrate-naïve cells. We concluded that removing TezRs and forming "Zero cells" altered the activity of genes or triggered genetic networks rearrangements. Therefore, we report for the first time that, by affecting TezRs, it is possible to control memory formation and "forgetting", both of which are critical aspects of memory regulation. This finding opens a wide range of possibilities for directed cellular programming [124].

To address the question of how TezRs network was formed, we hypothesized that this process involved different types of DNA and RNA transcription events. In support of this idea, we observed the inhibition of bacterial growth when cells lacking primary DNA-based TezRs (and not control cells) were treated with reverse transcriptase inhibitors. Accordingly, we speculated that this occurred due to the inhibition of TezR restoration by reverse transcriptases. Although reverse transcriptases have been found in a wide range of bacteria, their structure and function remain enigmatic [125, 126]. Moreover, bacterial retroelements with reverse transcription activity (mainly represented by group II introns associated with the CRISPR-Cas system), Abi-related reverse transcriptases, and retron reverse transcriptases encoding extrachromosomal multicopy single-stranded RNA/DNA structures all remain poorly understood [127–130].

We have not specifically investigated the mechanism of TezRs molecules translocation to the cell surface, but the observed upregulation of proteins associated with type VII secretion system (T7SS) following the loss of DNA-based TezRs alone or in combination with RNA-based TezRs, raises the question about T7SS involvement in translocation of DNA-based TezRs. Although, T7SS has not yet been fully characterized, and the intricate molecular mechanisms underlying its function remains elusive, the T7SS secretion machinery is attributed to bacterial pathogenicity and is also known to be a part of curli biogenesis machinery that requires extracellular DNA [131, 132].

Trying to answer the question of how the signal from TezRs was processed further downstream in the cells, we found that the integrase inhibitor raltegravir blocked the bacterial responses that was found to be controlled by TezRs such as dexamethasone utilization or response to heating. These results point out that bacterial recombinases might be implicated in the processing of stimuli from TezRs. Considering the findings together, we conclude that recombinases and reverse transcriptases are part of the TR-system.

Taking into consideration the nucleic acids-based chemical nature of TezRs, it is worthwhile revisiting some of the existing paradigms of microbiology associated with nucleic acids. Thus, some biological effects so far associated with the action of nucleases against bacterial biofilms and inhibition of bacterial adhesion, might actually stem from previously overlooked alterations to TezRs with subsequent loss of their receptive and regulatory function [64, 133]. Our data might also shed the light on the role of nucleic acids identified on cell surfaces, which have been described in some organisms but their contribution to cell functioning remained poorly defined [134–137].

The model used in this study and based on the use of nucleases to remove TezRs is relevant to natural conditions. Many bacteria secrete nucleases in the extracellular environment, suggesting that the destruction of TezRs may be a conserved and previously overlooked mechanism to gain a fitness advantage over competing strains [118, 138].

Along with the nucleases we used PI which is known to bind both DNA and RNA without penetrating live

cells and anti-DNA or anti-RNA antibodies [139]. As expected, bacteria following PI treatment behaved similarly as the "Drunk cells" after the destruction of primary DNA and RNA formed TezRs. And cells following treatment with anti-DNA or anti-RNA antibodies exhibited the same alterations of the regulation of their growth and activation of chemotaxis as those with TezRs destroyed with nucleases. Therefore, not only their destruction but also their inactivation due to PI binding could significantly affect the receptive and regulatory functions of TezRs.

Future studies of the TR-system will require the development of new tools, coupled with an interdisciplinary approach that bridges microbiology and molecular biology. They should focus on the structural aspects of TezRs, as well as the molecular mechanisms of their formation and translocation to the cell surface. The functioning of bacterial TezRs across different organisms, as well as the mechanisms of their interaction with ligands and signal transduction should also receive attention.

Considering the various cell features that are regulated by TezRs, we hypothesize that their specific functions stem from their physical characteristics, such as length and presence of specific loops or nucleic acids conformations [140, 141]. A better understanding of these properties could lead to further and more accurate subclassification of TezRs.

In follow-up studies, it will be critical to pay attention to the association of primary and secondary TezRs with the cell surface, and the way signals from these TezRs are transmitted further downstream in the cells. Based on our data, we speculate that secondary TezRs may exist as free receptors not bound to cell structures. However, we could not determine how TezRs interacted with protein receptors performing the same function. One can assume that some TezRs might be directly in contact with protein receptors, being an integral, sensing (i.e. ligand-binding) part of such a protein receptors. If so, TezRs should be present within different proteins receptors and not specific only for histidine kinases of a two-component regulatory system in bacteria because the identical biological effects were observed following the destruction of TezRs on mammalian cells that are known to lack a two-component regulatory system [45, 142].

Moreover, given the recently discovered ability of DNA molecules to modify and misfold proteins, it is intriguing whether TezRs could possess a similar chaperoning function [32, 143–145]. Recently, we discovered the existence of a similar regulatory system in eukaryotes [45]. Overall, this study is the first research that demonstrates the existence of TR-system in Gram-positive and Gram-negative bacteria which participates in recognition of environmental factors, remembering them and then obliterating the same. Although we are only starting to understand the regulatory roles of TR-system, as well as the structure of TezRs, the need to deepen our knowledge in this field does not diminish the importance of the present observations. We believe that upcoming studies will expand our understanding of the whole set of sensing and regulatory processes involving the TR-system.

Supplementary Information

The online version contains supplementary material available at https://doi.org/10.1186/s12934-022-01923-0.

Additional file 1: Table S1. Effect of primary TezR–D1/R1 removal on bacterial size

Additional file 2: Table S2. Effect of primary TezRs removal on the size of *B. pumilus* VT1200 biofilm

Additional file 3: Table S3. Effect of TezR removal on sporulation under normal conditions

Additional file 4: Table S4. Effect of TezR removal on sporulation under stress conditions

Additional file 5: Table S5. MICs of tested reverse transcriptase inhibitors and integrase inhibitor against control *S. aureus*

Additional file 6: Figure S1. Absence of RNase A internalization in *B. pumilus*

Additional file 7: Figure S2. Effect of TezRs removal on light sensing

Acknowledgements

We gratefully acknowledge Dr. You Zhou, Microscopy facility at the Center for Biotechnology in University of Nebraska-Lincoln for help in microscopy; Kristina Kardava, Marya Vecherkovskaya for setting some experiments, as well as Tatiana Lazareva; Genome Technology Center (GTC) for expert library preparation and sequencing, and the Applied Bioinformatics Laboratories (ABL) for providing bioinformatics support and helping with the analysis and interpretation of the data. GTC and ABL are shared resources partially supported by the Cancer Center Support Grant P30CA016087 at the Laura and Isaac Perlmutter Cancer Center. This work has used computing resources at the NYU School of Medicine High Performance Computing (HPC) Facility.

Author contributions

VT and GT designed experiments. VT and GT supervised data analysis, analyzed data and wrote the manuscript. All authors read and approved the final manuscript.

Funding

Not applicable.

Availability of data and materials

All the metagenomic datasets generated in this study are available upon request.

Declarations

Ethics approval and consent to participate

Not applicable.

Consent for publication

Not applicable.

Competing interests

The authors declare no competing interests.

Received: 24 August 2022 Accepted: 16 September 2022
Published online: 04 October 2022

References

1. Wadhams GH, Armitage JP. Making sense of it all: bacterial chemotaxis. Nat Rev Mol Cell Biol. 2004;5:1024–37.
2. Ortega Á, Zhulin IB, Krell T. Sensory repertoire of bacterial chemoreceptors. Microbiol Mol Biol Rev. 2017. https://doi.org/10.1128/MMBR.00033-17.
3. Bi S, Jin F, Sourjik V. Inverted signaling by bacterial chemotaxis receptors. Nat Commun. 2018;9:1–13.
4. Bretl DJ, Demetriadou C, Zahrt TC. Adaptation to environmental stimuli within the host: two-component signal transduction systems of *Mycobacterium tuberculosis*. Microbiol Mol Biol Rev. 2011;75:566–82.
5. Gao R, Mack TR, Stock AM. Bacterial response regulators: versatile regulatory strategies from common domains. Trends Biochem Sci. 2007;32:225–34.
6. Stock AM, Mottonen JM, Stock JB, Schutt CE. Three-dimensional structure of CheY, the response regulator of bacterial chemotaxis. Nature. 1989;337:745–9.
7. Mascher T, Helmann JD, Unden G. Stimulus perception in bacterial signal-transducing histidine kinases. Microbiol Mol Biol Rev. 2006;70:910–38.
8. Mitrophanov AY, Groisman EA. Signal integration in bacterial two-component regulatory systems. Genes Dev. 2008;22:2601–11.
9. Rayo J, Amara N, Krief P, Meijler MM. Live cell labeling of native intracellular bacterial receptors using aniline-catalyzed oxime ligation. J Am Chem Soc. 2011;133:7469–75.
10. Falke JJ, Hazelbauer GL. Transmembrane signaling in bacterial chemoreceptors. Trends Biochem Sci. 2001;26:257–65.
11. Ng W-L, et al. Probing bacterial transmembrane histidine kinase receptor-ligand interactions with natural and synthetic molecules. Proc Natl Acad Sci. 2010;107:5575–80.
12. Falke JJ. Cooperativity between bacterial chemotaxis receptors. Proc Natl Acad Sci. 2002;99:6530–2.
13. Hazelbauer GL, Falke JJ, Parkinson JS. Bacterial chemoreceptors: high-performance signaling in networked arrays. Trends Biochem Sci. 2008;33:9–19.
14. Yang Y, Sourjik V. Opposite responses by different chemoreceptors set a tunable preference point in *Escherichia coli* pH taxis. Mol Microbiol. 2012;86:1482–9.
15. Machuca MA, et al. Helicobacter pylori chemoreceptor TlpC mediates chemotaxis to lactate. Sci Rep. 2017;7:1–15.
16. Li H, Wang H. Activation of xenobiotic receptors: driving into the nucleus. Expert Opin Drug Metab Toxicol. 2010;6:409–26.
17. Sourjik V, Berg HC. Functional interactions between receptors in bacterial chemotaxis. Nature. 2004;428:437–41.
18. Jacquin J, et al. Microbial ecotoxicology of marine plastic debris: a review on colonization and biodegradation by the "Plastisphere." Front Microbiol. 2019. https://doi.org/10.3389/fmicb.2019.00865.
19. Wolf DM, et al. Memory in microbes: quantifying history-dependent behavior in a bacterium. PLoS ONE. 2008. https://doi.org/10.1371/journal.pone.0001700.
20. Kordes A, et al. Establishment of an induced memory response in *Pseudomonas aeruginosa* during infection of a eukaryotic host. ISME J. 2019;13:2018–30.
21. Gosztolai A, Barahona M. Cellular memory enhances bacterial chemotactic navigation in rugged environments. Commun Phys. 2020;3:1–10.
22. Andersson SGE. Stress management strategies in single bacterial cells. Proc Natl Acad Sci. 2016;113:3921–3.
23. Lambert G, Kussell E. Memory and fitness optimization of bacteria under fluctuating environments. PLoS Genet. 2014. https://doi.org/10.1371/journal.pgen.1004556.
24. Stock JB, Zhang S. The biochemistry of memory. Curr Biol. 2013;23:R741–5.
25. Vashistha H, Kohram M, Salman H. Non-genetic inheritance restraint of cell-to-cell variation. Elife. 2021. https://doi.org/10.7554/eLife.64779.
26. Yang C-Y, et al. Encoding membrane-potential-based memory within a microbial community. Cell Syst. 2020;10:417–23.
27. Matsunaga T, et al. Complete genome sequence of the facultative anaerobic magnetotactic bacterium *Magnetospirillum* sp. strain AMB-1. DNA Res. 2005;12:157–66.
28. McCausland HC, Komeili A. Magnetic genes: studying the genetics of biomineralization in magnetotactic bacteria. PLOS Genet. 2020. https://doi.org/10.1371/journal.pgen.1008499.
29. Scheffel A, et al. An acidic protein aligns magnetosomes along a filamentous structure in magnetotactic bacteria. Nature. 2006;440:110–4.
30. Nordmann GC, Hochstoeger T, Keays DA. Magnetoreception—a sense without a receptor. PLOS Biol. 2017. https://doi.org/10.1371/journal.pbio.2003234.
31. Monteil CL, Lefevre CT. Magnetoreception in microorganisms. Trends Microbiol. 2020;28:266–75.
32. Blank M, Goodman R. DNA is a fractal antenna in electromagnetic fields. Int J Radiat Biol. 2011;87:409–15.
33. Berashevich J, Chakraborty T. How the surrounding water changes the electronic and magnetic properties of DNA. J Phys Chem B. 2008;112:14083–9.
34. Nikiforov VN, Koksharov YA, Irkhin VY. Magnetic properties of "doped" DNA. J Magn Magn Mater. 2018;459:340–4.
35. Yoney A, Salman H. Precision and variability in bacterial temperature sensing. Biophys J. 2015;108:2427–36.
36. Chursov A, Kopetzky SJ, Bocharov G, Frishman D, Shneider A. RNAtips: analysis of temperature-induced changes of RNA secondary structure. Nucleic Acids Res. 2013;41:W486–91.
37. Sengupta P, Garrity P. Sensing temperature. Curr Biol. 2013;23:R304–7.
38. Barria C, Malecki M, Arraiano CM. Bacterial adaptation to cold. Microbiology. 2013;159:2437–43.
39. Abatedaga I, et al. Integration of temperature and blue-light sensing in *Acinetobacter baumannii* through the BlsA sensor. Photochem Photobiol. 2017;93:805–14.
40. Golic AE, et al. BlsA Is a Low to moderate temperature blue light photoreceptor in the human pathogen *Acinetobacter baumannii*. Front Microbiol. 2019. https://doi.org/10.3389/fmicb.2019.01925.
41. Briegel A, et al. New Insights into bacterial chemoreceptor array structure and assembly from electron cryotomography. Biochemistry. 2014;53:1575–85.
42. Bi S, Sourjik V. Stimulus sensing and signal processing in bacterial chemotaxis. Curr Opin Microbiol. 2018;45:22–9.
43. Parkinson JS, Hazelbauer GL, Falke JJ. Signaling and sensory adaptation in *Escherichia coli* chemoreceptors: 2015 update. Trends Microbiol. 2015;23:257–66.
44. Beyer J, Szöllössi A, Byles E, Fischer R, Armitage J. Mechanism of signalling and adaptation through the *Rhodobacter sphaeroides* cytoplasmic chemoreceptor cluster. Int J Mol Sci. 2019. https://doi.org/10.3390/ijms20205095.
45. Tetz V, Tetz G. Novel cell receptor system of eukaryotes formed by previously unknown nucleic acid-based receptors. Receptors. 2022;1:13–53. https://doi.org/10.3390/receptors1010003.
46. Greenfield EA. Standard immunization of rabbits. Cold Spring Harb Protoc. 2020. https://doi.org/10.1101/pdb.prot100305.
47. Schindelin J, et al. Fiji: an open-source platform for biological-image analysis. Nat Methods. 2012;9:676–82.
48. Rueden CT, et al. Image J2: ImageJ for the next generation of scientific image data. BMC Bioinformatics. 2017;18:1–26.
49. Wang X, et al. Hyaluronic acid modification of RNase A and its intracellular delivery using lipid-like nanoparticles. J Control Release. 2017;263:39–45.
50. Hulsen T, de Vlieg J, Alkema W. BioVenn – a web application for the comparison and visualization of biological lists using area-proportional Venn diagrams. BMC Genomics. 2008;9(488):1–6.
51. Golding I. Single-cell studies of phage λ: hidden treasures under Occam's Rug. Annu Rev Virol. 2016;3:453–72.
52. Svenningsen MS, Veress A, Harms A, Mitarai N, Semsey S. Birth and resuscitation of (p)ppGpp induced antibiotic tolerant persister cells. Sci Rep. 2019;9(6056):1–13.
53. Manukumar HM, Umesha S. MALDI-TOF-MS based identification and molecular characterization of food associated methicillin-resistant *Staphylococcus aureus*. Sci Rep. 2017;7:1–16.

54. Bennett RW, Monday SR. S aureus. In: Miliotis BJ, editor. International handbook of foodborne pathogens. Boca Raton: CRC Press; 2003. p. 41–59.
55. *Guide for the Care and Use of Laboratory Animals*. (National Academies Press, 1996). doi:https://doi.org/10.17226/5140.
56. Choudhry P. High-throughput method for automated colony and cell counting by digital image analysis based on edge detection. PLoS ONE. 2016. https://doi.org/10.1371/journal.pone.0148469.
57. Jones ME, Thomas SM, Rogers A. Luria-Delbrück fluctuation experiments: design and analysis. Genetics. 1994;136:1209–16.
58. Paliy O, Gunasekera TS. Growth of *E. coli* BL21 in minimal media with different gluconeogenic carbon sources and salt contents. Appl Microbiol Biotechnol. 2007;73:1169–72.
59. Fernández de las Heras L, García Fernández E, María Navarro Llorens J, Perera J, Drzyzga O. Morphological, physiological, and molecular characterization of a newly isolated steroid-degrading actinomycete, identified as *Rhodococcus* ruber strain Chol-4. Curr Microbiol. 2009;59:548–53.
60. Zhu L, Yang Z, Yang Q, Tu Z, Ma L, Shi Z, Li X. Degradation of dexamethasone by acclimated strain of *Pseudomonas alcaligenes*. Int J Clin Exp Med. 2015;8(10971):10971.
61. Bohn C, et al. Experimental discovery of small RNAs in *Staphylococcus aureus* reveals a riboregulator of central metabolism. Nucleic Acids Res. 2010;38:6620–36.
62. Kengmo Tchoupa A, et al. The type VII secretion system protects *Staphylococcus aureus* against antimicrobial host fatty acids. Sci Rep. 2020;10:14838.
63. Taylor JC, et al. A type VII secretion system of *Streptococcus gallolyticus* subsp. gallolyticus contributes to gut colonization and the development of colon tumors. PLOS Pathog. 2021;17:e1009182. https://doi.org/10.1371/journal.ppat.1009182.
64. Whitchurch CB, Tolker-Nielsen T, Ragas PC, Mattick JS. Extracellular DNA required for bacterial biofilm formation. Science. 2022;295:1487–1487.
65. Ingham CJ, Jacob E. Swarming and complex pattern formation in *Paenibacillus vortex* studied by imaging and tracking cells. BMC Microbiol. 2008;8:1–16.
66. Kampers LF, et al. A metabolic and physiological design study of *Pseudomonas putida* KT2440 capable of anaerobic respiration. BMC Microbiol. 2021;21:1–15.
67. Glasser NR, Kern SE, Newman DK. Phenazine redox cycling enhances anaerobic survival in *P seudomonas aeruginosa* by facilitating generation of ATP and a proton-motive force. Mol Microbiol. 2014;92:399–412.
68. Nikel PI, de Lorenzo V. Engineering an anaerobic metabolic regime in *Pseudomonas putida* KT2440 for the anoxic biodegradation of 1,3-dichloroprop-1-ene. Metab Eng. 2013;15:98–112.
69. Eschbach M, et al. Long-term anaerobic survival of the opportunistic pathogen *Pseudomonas aeruginosa* via pyruvate fermentation. J Bacteriol. 2004;186:4596–604.
70. Fuchs S, Pané-Farré J, Kohler C, Hecker M, Engelmann S. Anaerobic gene expression in *Staphylococcus aureus*. J Bacteriol. 2007;189:4275–89.
71. Kadowaki T, et al. *Porphyromonas gingivalis* proteinases as virulence determinants in progression of periodontal diseases. J Biochem. 2000;128:153–9.
72. Saunders SH, et al. Extracellular DNA promotes efficient extracellular electron transfer by pyocyanin in *Pseudomonas aeruginosa* biofilms. Cell. 2020;182:919–32.
73. Ciemniecki JA, Newman DK. The potential for redox-active metabolites to enhance or unlock anaerobic survival metabolisms in aerobes. J Bacteriol. 2020. https://doi.org/10.1128/JB.00797-19.
74. Rashid MH, Kornberg A. Inorganic polyphosphate is needed for swimming, swarming, and twitching motilities of *Pseudomonas aeruginosa*. Proc Natl Acad Sci. 2000;97:4885–90.
75. Fraser GM, Hughes C. Swarming motility. Curr Opin Microbiol. 1999;2:630–5.
76. Hagai E, et al. Surface-motility induction, attraction and hitchhiking between bacterial species promote dispersal on solid surfaces. ISME J. 2014;8:1147–51.
77. Abee T, Kovács ÁT, Kuipers OP, van der Veen S. Biofilm formation and dispersal in Gram-positive bacteria. Curr Opin Biotechnol. 2011;22:172–9.
78. Bartolini M, et al. Regulation of biofilm aging and dispersal in *Bacillus subtilis* by the alternative sigma factor SigB. J Bacteriol. 2019. https://doi.org/10.1128/JB.00473-18.
79. McDougald D, Rice SA, Barraud N, Steinberg PD, Kjelleberg S. Should we stay or should we go: mechanisms and ecological consequences for biofilm dispersal. Nat Rev Microbiol. 2012;10:39–50.
80. Velasco E, et al. A new role for Zinc limitation in bacterial pathogenicity: modulation of α-hemolysin from uropathogenic *Escherichia coli*. Sci Rep. 2018;8:1–11.
81. Huang YJ, Begley L. C32 LUNG INJURY, ARDS, AND SEPSIS: the effects of inhaled glucocorticoids on growth of *Pseudomonas* AerugINOSa. Am J Respir Crit Care Med. 2017;195:A5233.
82. DeNiro M, Epstein S. Mechanism of carbon isotope fractionation associated with lipid synthesis. Science. 1977;197:261–3.
83. Basan M, et al. A universal trade-off between growth and lag in fluctuating environments. Nature. 2020;584:470–4.
84. Shibasaki H, Tanabe C, Furuta T, Kasuya Y. Hydrolysis of conjugated steroids by the combined use of β-glucuronidase preparations from helix pomatia and ampullaria: determination of urinary cortisol and its metabolites. Steroids. 2001;66:795–801.
85. Zarkan A, et al. Indole pulse signalling regulates the cytoplasmic pH of *E. coli* in a memory-like manner. Sci Rep. 2019;9:1–10.
86. Lyon P. The cognitive cell: bacterial behavior reconsidered. Front Microbiol. 2015;6:264.
87. García-López V, et al. Molecular machines open cell membranes. Nature. 2017;548:567–72.
88. Szilvay AM, Stern B, Blichenberg A, Helland DE. Structural and functional similarities between HIV-1 reverse transcriptase and the *Escherichia coli* RNA polymerase β′ subunit. FEBS Lett. 2000;484:43–7.
89. Sciamanna I, De Luca C, Spadafora C. The reverse transcriptase encoded by LINE-1 retrotransposons in the genesis, progression, and therapy of cancer. Front Chem. 2016;4:6.
90. Spanopoulou E, et al. The homeodomain region of Rag-1 reveals the parallel mechanisms of bacterial and V(D)J recombination. Cell. 1996;87:263–76.
91. Nishana M, Nilavar NM, Kumari R, Pandey M, Raghavan SC. HIV integrase inhibitor, Elvitegravir, impairs RAG functions and inhibits V(D)J recombination. Cell Death Dis. 2017. https://doi.org/10.1038/cddis.2017.237.
92. Hershko A, Ciechanover A. The ubiquitin system. Annu Rev Biochem. 1998;67:425–79.
93. Joyce GF. RNA evolution and the origins of life. Nature. 1989;338:217–24.
94. MartÃ-nez LC, Vadyvaloo V. Mechanisms of post-transcriptional gene regulation in bacterial biofilms. Front Cell Infect Microbiol. 2014. https://doi.org/10.3389/fcimb.2014.00038.
95. Kearns DB. A field guide to bacterial swarming motility. Nat Rev Microbiol. 2010;8:634–44.
96. Claessen D, Rozen DE, Kuipers OP, Søgaard-Andersen L, van Wezel GP. Bacterial solutions to multicellularity: a tale of biofilms, filaments and fruiting bodies. Nat Rev Microbiol. 2014;12:115–24.
97. Kaplan JB. Biofilm dispersal: mechanisms, clinical implications, and potential therapeutic uses. J Dent Res. 2010;89:205–18.
98. Güvener ZT, Harwood CS. Subcellular location characteristics of the *Pseudomonas aeruginosa* GGDEF protein, WspR, indicate that it produces cyclic-di-GMP in response to growth on surfaces. Mol Microbiol. 2007. https://doi.org/10.1111/j.1365-2958.2007.06008.x.
99. Dubnau D, Losick R. Bistability in bacteria. Mol Microbiol. 2006;61:564–72.
100. Wilmaerts D, Windels EM, Verstraeten N, Michiels J. General mechanisms leading to persister formation and awakening. Trends Genet. 2019;35:401–11.
101. Loh E, Righetti F, Eichner H, Twittenhoff C, Narberhaus F. RNA thermometers in bacterial pathogens. Microbiol Spectr. 2018;6:6–12.
102. Krishna S, Maslov S, Sneppen K. UV-induced mutagenesis in *Escherichia coli* SOS response: a quantitative model. PLoS Comput Biol. 2007;3: e41. https://doi.org/10.1371/journal.pcbi.0030041.
103. Wadhawan S, Gautam S. Rescue of *Escherichia coli* cells from UV-induced death and filamentation by caspase-3 inhibitor. Int Microbiol. 2019;22:369–76.

104. Erental A, Kalderon Z, Saada A, Smith Y, Engelberg-Kulka H. Apoptosis-like death, an extreme SOS response in *Escherichia coli*. MBio. 2014. https://doi.org/10.1128/mBio.01426-14.
105. Michel B. After 30 years of study, the bacterial SOS response still surprises us. PLoS Biol. 2005;3: e255. https://doi.org/10.1371/journal.pbio.0030255.
106. Kreuzer KN. DNA damage responses in prokaryotes: regulating gene expression, modulating growth patterns, and manipulating replication forks. Cold Spring Harb Perspect Biol. 2013;5:a012674–a012674.
107. Tetz G, Tetz V. Introducing the sporobiota and sporobiome. Gut Pathog. 2017;9(38):1–6.
108. Errington J. Regulation of endospore formation in *Bacillus subtilis*. Nat Rev Microbiol. 2003;1:117–26.
109. Irkhin VY, Nikiforov VN. Quantum effects and magnetism in the spatially distributed DNA molecules. J Magn Magn Mater. 2018;459:345–9.
110. Savelyev IV, Zyryanova NV, Polesskaya OO, Myakishev-Rempel M. On the existence of the DNA resonance code and its possible mechanistic connection to the neural code. NeuroQuantology. 2019;17(2):56.
111. Yi J. Emergent paramagnetism of DNA molecules. Phys Rev B. 2006;74:212406. https://doi.org/10.1103/PhysRevB.74.212406.
112. Montagnier L, Aïssa J, Ferris S, Montagnier J-L, Lavalléee C. Electromagnetic signals are produced by aqueous nanostructures derived from bacterial DNA sequences. Interdiscip Sci Comput Life Sci. 2009;1:81–90.
113. Zhang Q, Throolin R, Pitt SW, Serganov A, Al-Hashimi HM. Probing motions between equivalent RNA domains using magnetic field induced residual dipolar couplings: accounting for correlations between motions and alignment. J Am Chem Soc. 2003;125:10530–1.
114. Briegel A, et al. Structure of bacterial cytoplasmic chemoreceptor arrays and implications for chemotactic signaling. Elife. 2014. https://doi.org/10.7554/eLife.02151.
115. Schaaper RM, Dunn RL. Spectra of spontaneous mutations in *Escherichia coli* strains defective in mismatch correction: the nature of in vivo DNA replication errors. Proc Natl Acad Sci. 1987;84:6220–4.
116. Canchaya C, Fournous G, Chibani-Chennoufi S, Dillmann M-L, Brüssow H. Phage as agents of lateral gene transfer. Curr Opin Microbiol. 2003;6:417–24.
117. Yang D, et al. Human ribonuclease A superfamily members, eosinophil-derived neurotoxin and pancreatic ribonuclease, induce dendritic cell maturation and activation. J Immunol. 2004;173:6134–42.
118. Sumby P, et al. Extracellular deoxyribonuclease made by group A *Streptococcus* assists pathogenesis by enhancing evasion of the innate immune response. Proc Natl Acad Sci. 2005;102:1679–84.
119. Lux R, Jahreis K, Bettenbrock K, Parkinson JS, Lengeler JW. Coupling the phosphotransferase system and the methyl-accepting chemotaxis protein-dependent chemotaxis signaling pathways of *Escherichia coli*. Proc Natl Acad Sci. 1995;92:11583–7.
120. Sheth RU, Wang HH. DNA-based memory devices for recording cellular events. Nat Rev Genet. 2018;19:718–32.
121. Kurosaki T, Kometani K, Ise W. Memory B cells. Nat Rev Immunol. 2015;15:149–59.
122. McHeyzer-Williams M, Okitsu S, Wang N, McHeyzer-Williams L. Molecular programming of B cell memory. Nat Rev Immunol. 2012;12:24–34.
123. Raychaudhuri S. The problem of antigen affinity discrimination in B-cell immunology. ISRN Biomath. 2013;2013:1–18.
124. Chowdhury S, et al. Programmable bacteria induce durable tumor regression and systemic antitumor immunity. Nat Med. 2019;25:1057–63.
125. Berg P, Kornberg RD, Fancher H, Dieckmann M. Competition between RNA polymerase and DNA polymerase for the DNA template. Biochem Biophys Res Commun. 1965;18:932–42.
126. Lim D, Maas WK. Reverse transcriptase in bacteria. Mol Microbiol. 1989;3:1141–4.
127. Toro N, Martínez-Abarca F, González-Delgado A. The reverse transcriptases associated with CRISPR-Cas systems. Sci Rep. 2017;7:1–7.
128. Toro N, Nisa-Martínez R. Comprehensive phylogenetic analysis of bacterial reverse transcriptases. PLoS ONE. 2014;9: e114083. https://doi.org/10.1371/journal.pone.0114083.
129. Lampson BC, Inouye M, Inouye S. Retrons, msDNA, and the bacterial genome. Cytogenet Genome Res. 2005;110:491–9.
130. Simon DM, Zimmerly S. A diversity of uncharacterized reverse transcriptases in bacteria. Nucleic Acids Res. 2008;36:7219–29.
131. Guerrier-Takada C, Gardiner K, Marsh T, Pace N, Altman S. The RNA moiety of ribonuclease P is the catalytic subunit of the enzyme. Cell. 1983;35:849–57.
132. Huang N, et al. Natural display of nuclear-encoded RNA on the cell surface and its impact on cell interaction. Genome Biol. 2020;21(225):1–23.
133. Tetz GV, Artemenko NK, Tetz VV. Effect of DNase and antibiotics on biofilm characteristics. Antimicrob Agents Chemother. 2009. https://doi.org/10.1128/AAC.00471-08.
134. Huang N, et al. Natural display of nuclear-encoded RNA on the cell surface and its impact on cell interaction. Genome Biol. 2020;21:1–23.
135. Doyle RJ, Koch AL, Carstens PH. Cell wall-DNA association in *Bacillus subtilis*. J Bacteriol. 1983;153:1521–7.
136. Hall MR, Meinke W, Goldstein DA, Lerner RA. Synthesis of cytoplasmic membrane-associated DNA in lymphocyte nucleus. Nat New Biol. 1971;234:227–9.
137. Molan K, Žgur Bertok D. Small prokaryotic DNA-binding proteins protect genome integrity throughout the life cycle. Int J Mol Sci. 2022;23:4008. https://doi.org/10.3390/ijms23074008.
138. Terekhov SS, et al. A kinase bioscavenger provides antibiotic resistance by extremely tight substrate binding. Sci Adv. 2020. https://doi.org/10.1126/sciadv.aaz986.
139. Rosenberg M, Azevedo NF, Ivask A. Propidium iodide staining underestimates viability of adherent bacterial cells. Sci Rep. 2019;9(6483):1–12.
140. Bacolla A, Wang G, Vasquez KM. New perspectives on DNA and RNA triplexes as effectors of biological activity. PLOS Genet. 2015;11: e1005696. https://doi.org/10.1371/journal.pgen.1005696.
141. Herbert A, et al. Special issue: A, B and Z: the structure, function and genetics of Z-DNA and Z-RNA. Int J Mol Sci. 2021;22:7686.
142. Ibrahim IM, Puthiyaveetil S, Allen JF. A two-component regulatory system in transcriptional control of photosystem stoichiometry: redox-dependent and sodium ion-dependent phosphoryl transfer from cyanobacterial histidine kinase Hik2 to response regulators Rre1 and RppA. Front Plant Sci. 2016. https://doi.org/10.3389/fpls.2016.00137.
143. Tetz G, Tetz V. Bacterial extracellular DNA promotes β-amyloid aggregation. Microorganisms. 2021. https://doi.org/10.3390/microorganisms9061301.
144. Tetz G, et al. Bacterial DNA promotes Tau aggregation. Sci Rep. 2020. https://doi.org/10.1038/s41598-020-59364-x.
145. Tetz V, Tetz G. Bacterial DNA induces the formation of heat-resistant disease-associated proteins in human plasma. Sci Rep. 2019. https://doi.org/10.1038/s41598-019-54618-9.

Publisher's Note

Springer Nature remains neutral with regard to jurisdictional claims in published maps and institutional affiliations.

Ready to submit your research? Choose BMC and benefit from:

- fast, convenient online submission
- thorough peer review by experienced researchers in your field
- rapid publication on acceptance
- support for research data, including large and complex data types
- gold Open Access which fosters wider collaboration and increased citations
- maximum visibility for your research: over 100M website views per year

At BMC, research is always in progress.

Learn more biomedcentral.com/submissions

BMC